

Rothamsted Repository Download

A - Papers appearing in refereed journals

Brambilla, V., Martignago, D., Goretti, D., Cerise, M., Somssich, M., de Rosa, M., Galbiati, F., Shrestha, R., Lazzaro, F., Simon, R. and Fornara, F. 2017. Antagonistic Transcription Factor Complexes Modulate the Floral Transition in Rice. *The Plant Cell*. 29 (11), pp. 2801-2816.

The publisher's version can be accessed at:

- <https://dx.doi.org/10.1105/tpc.17.00645>

The output can be accessed at: <https://repository.rothamsted.ac.uk/item/8v538>.

© 17 October 2017, Rothamsted Research. Licensed under the Creative Commons CC BY.

1 **RESEARCH ARTICLE**

2 **Antagonistic Transcription Factor Complexes Modulate the Floral Transition in**
3 **Rice**

4 **Vittoria Brambilla^{1,2}, Damiano Martignago^{1,3}, Daniela Goretti^{1,4}, Martina Cerise¹, Marc Somssich^{5,6}, Matteo**
5 **de Rosa⁷, Francesca Galbiati¹, Roshni Shrestha^{1,9}, Federico Lazzaro¹, Rüdiger Simon⁵ and Fabio Fornara^{1,*}**
6

7 ¹ University of Milan, Department of Biosciences, 20133 Milano, Italy

8 ² University of Milan, Department of Agricultural and Environmental Sciences, 20133 Milano, Italy.

9 ³ Present address: Department of Plant Biology and Crop Science, Rothamsted Research, Harpenden, Herts, United
10 Kingdom

11 ⁴ Present address: Umeå Plant Science Centre, Department of Plant Physiology, Umeå University, Umeå,
12 Sweden

13 ⁵ Institute for Developmental Genetics and Cluster of Excellence on Plant Sciences, Heinrich Heine University,
14 Universitätsstr. 1, D-40225 Düsseldorf, Germany

15 ⁶ Present address: School of Biosciences, the University of Melbourne, 3010 Victoria, Australia

16 ⁷ CNR-Biophysics Institute, Via Celoria 26, 20133, Milano, Italy

17 ⁹ Present address: Institute of Biological and Environmental Sciences, University of Aberdeen, Aberdeen AB24
18 3UU, UK

19 *Corresponding author: fabio.fornara@unimi.it
20

21 **Short title:** Antagonistic flowering complexes in rice

22 **One-sentence summary:** Rice flowering depends on formation of transcriptional complexes, some of which act
23 at the shoot apical meristem, whereas others promote or repress the floral transition by acting from the leaves.

24 The author responsible for distribution of materials integral to the findings presented in this article in accordance
25 with the policy described in the Instructions for Authors (www.plantcell.org) is Fabio Fornara
26 (fabio.fornara@unimi.it).

27
28 **ABSTRACT**

29 Plants measure day or night lengths to coordinate specific developmental changes with a favorable season. In rice
30 (*Oryza sativa*), the reproductive phase is initiated by exposure to short days when expression of *HEADING DATE*
31 *3a* (*Hd3a*) and *RICE FLOWERING LOCUS T 1* (*RFT1*) is induced in leaves. The cognate proteins are components
32 of the florigenic signal, and move systemically through the phloem to reach the shoot apical meristem (SAM). In
33 the SAM, they form a transcriptional activation complex with the bZIP transcription factor OsFD1, to start panicle
34 development. Here, we show that Hd3a and RFT1 can form transcriptional activation or repression complexes also
35 in leaves, and feed-back to regulate their own transcription. Activation complexes depend upon OsFD1 to promote
36 flowering. However, additional bZIPs, including Hd3a BINDING REPRESSOR FACTOR 1 (HBF1) and HBF2
37 form repressor complexes that reduce *Hd3a* and *RFT1* expression to delay flowering. We propose that Hd3a and
38 RFT1 are also active locally in leaves to fine-tune photoperiodic flowering responses.
39

40 INTRODUCTION

41 The floral transition sets the beginning of the reproductive phase and is completed upon switching of the
42 shoot apical meristem (SAM) from indeterminate vegetative to determinate reproductive growth. In
43 many plant species, these changes are triggered by day length (or photoperiod), which is measured in
44 leaves to synchronize inflorescence development with the most favorable seasons. This signaling
45 mechanism requires systemic communication signals that integrate environmental inputs and connect
46 distant tissues of the plant.

47 Rice (*Oryza sativa*) preferentially flowers under short days (SD). When day length falls under a critical
48 threshold, proteins encoded by the *HEADING DATE 3a* (*Hd3a*) and *RICE FLOWERING LOCUS T 1*
49 (*RFT1*) loci are produced in leaves and delivered through the phloem to the SAM, where they induce
50 developmental reprogramming (Tamaki et al., 2007, 2015; Komiya et al., 2009). Both proteins share
51 homology with FLOWERING LOCUS T (FT) of Arabidopsis, and belong to the
52 phosphatidylethanolamine binding protein (PEBP) family of regulators, which includes also
53 TERMINAL FLOWER 1 (TFL1) homologues (Kojima et al., 2002; Ho and Weigel, 2014). However,
54 whereas FT-like proteins are strong activators of flowering, TFL1-like proteins are flowering inhibitors
55 (Wickland and Hanzawa, 2015).

56 Under inductive photoperiods, both *Hd3a* and *RFT1* are transcribed, and their protein products are
57 essential for flowering to the extent that artificial reduction of their mRNA expression results in never-
58 flowering plants (Komiya et al., 2008; Tamaki et al., 2015). However, transcription of *RFT1* can be
59 induced also under long days (LD), and its floral promotive activity under these conditions contributes
60 to the facultative nature of the photoperiodic flowering response of rice (Gómez-Ariza et al., 2015;
61 Komiya et al., 2009).

62 Induction of *Hd3a* and *RFT1* expression in leaves results from the integration of photoperiodic
63 information with diurnal timing set by the circadian clock. Environmental signals ultimately converge
64 on the transcriptional activation of *Early heading date 1* (*Ehd1*), encoding a B-type response regulator
65 unique to rice (Brambilla and Fornara, 2013; Doi et al., 2004; Cho et al., 2016). Transcription of *Ehd1*,
66 *Hd3a* and *RFT1* thus correlates under SD in leaves, showing a transient induction that persists only for
67 the time required to irreversibly commit flowering at the SAM (Galbiati et al., 2016; Doi et al., 2004;
68 Cho et al., 2016; Komiya et al., 2008). Once a sufficient amount of Hd3a and/or RFT1 proteins reaches
69 the SAM, expression of target genes that promote inflorescence formation is induced (Taoka et al., 2011;
70 Tamaki et al., 2015).

71 FT-like proteins have no DNA binding property. Therefore, upon reaching the cytoplasm of cells at the

72 SAM, they bind to transcription factors of the bZIP family, including FD in Arabidopsis and OsFD1 in
73 rice (Wigge et al., 2005; Taoka et al., 2011). The complex, originally found to be dimeric based on studies
74 in Arabidopsis, was later demonstrated to contain also a 14-3-3 protein of the Gf14 family (G-box factor
75 14-3-3) that bridges the interaction between OsFD1 and Hd3a. The resulting ternary complex, named
76 florigen activation complex (FAC) is targeted to the nucleus where it further dimerizes, forming a
77 heterohexameric complex tethered by OsFD1 on target DNA sequences (Zhao et al., 2015; Taoka et al.,
78 2011). Similar interactions take place in many plant species, including tomato (Park et al., 2014), potato
79 (Teo et al., 2017), wheat and barley (Li et al., 2015), maize (Danilevskaya et al., 2008), and hybrid aspen
80 (Tylewicz et al., 2015), suggesting that this molecular module is widely conserved among Angiosperms.
81 This conservation is further corroborated by inter-specific interactions demonstrated to occur between
82 Hd3a/RFT1 and FD (Jang et al., 2017). In many such examples, FD-like genes can provide DNA binding
83 specificity by recognizing ACGT-containing consensus sequences on the DNA of target promoters
84 (Izawa et al., 1993; Li and Dubcovsky, 2008; Taoka et al., 2011; Wigge et al., 2005). Competition
85 between FT-like and TFL1-like proteins for interaction with FD and 14-3-3 proteins partly explains their
86 opposite function on flowering and shoot architecture. Again, such competitive behavior is widespread
87 among Angiosperms (Pnueli et al., 2001; Randoux et al., 2014; Hanano and Goto, 2011; Park et al.,
88 2014).

89 The rice genome encodes seven Gf14 proteins, four of which (the b, c, d and e) can assemble into a FAC
90 (Taoka et al., 2011). The Gf14c protein was the first to be functionally characterized as an Hd3a interactor
91 (Purwestri et al., 2009; Taoka et al., 2011). Because of their redundancy and pleiotropic effects, it has
92 not been possible to study *gf14* mutants, but transgenic rice overexpressing *Gf14c* had delayed flowering
93 (Purwestri et al., 2009). Despite the apparent contrast with the nature of a FAC, this result might indicate
94 that a tightly regulated balance between FAC components needs to be achieved at the SAM to promote
95 flowering. Alternatively, floral repressor complexes containing Gf14c might exist and become
96 predominant upon overexpression of this specific 14-3-3 protein.

97 Besides FD-like transcription factors and 14-3-3 proteins, FT-like genes can interact with members of
98 the TEOSINTE BRANCHED1, CYCLOIDEA, PCF (TCP) transcription factor family. The ability to
99 bind distinct members of this group of regulators partly discriminates between FT- and TFL1-like
100 proteins, and indicates that TCPs are preferential interactors of FT-like proteins (Mimida et al., 2011;
101 Niwa et al., 2013; Ho and Weigel, 2014). Finally, apple Vascular Plant One Zinc finger (MdVOZ1a) was
102 isolated as an interactor of apple FT and shown to alter inflorescence architecture when expressed in
103 Arabidopsis (Mimida et al., 2011). Whether interactions between FT-like and VOZ-like proteins are

104 conserved among flowering plants is yet to be assessed.
105 Downstream targets of the FAC at the SAM include members of the MADS-box transcription factor
106 family that are necessary to switch the meristem to reproductive growth. In Arabidopsis, induction of
107 *SUPPRESSOR OF OVEREXPRESSION OF CONSTANS 1 (SOC1)*, *FRUITFULL (FUL)* and *APETALA*
108 *1 (API)* takes place shortly after arrival of FT at the SAM (Andrés and Coupland, 2012). Similarly,
109 *OsMADS14*, *OsMADS15* and *OsMADS18*, genes belonging the *FUL* clade, and *OSMADS34/PAP2*, a
110 *SEPALLATA (SEP)*-like gene, are progressively activated upon floral transition in rice (Kobayashi et al.,
111 2012; Litt and Irish, 2003). Mutants in which all four genes are silenced develop inflorescence stems
112 where flowers are replaced by vegetative shoots (Kobayashi et al., 2012). This general mode of action of
113 the florigens at the SAM has been observed in several plant species (Jang et al., 2015; Jaudal et al., 2015;
114 Li and Dubcovsky, 2008). However, FACs can be deployed also in tissues different from the SAM, to
115 control a broad spectrum of developmental processes different from inflorescence formation. For
116 example, components of FACs governing leaf development have been reported in both Arabidopsis and
117 rice (Teper-Bamnolker and Samach, 2005; Tsuji et al., 2013). Potato tuber formation depends on FACs
118 forming at the stolon meristem in response to FT export from the leaves (Navarro et al., 2011; Teo et al.,
119 2017). Seasonal growth cessation in trees is induced by FACs assembled in vegetative apical meristems
120 that stop elongation and leaf production before the onset of winter (Tylewicz et al., 2015). These findings
121 illustrate the plasticity and robustness of FACs as integrators of photoperiodic signals into distinct
122 developmental networks.

123 Given the high number of OsbZIP-coding genes in rice, the combinatorial interactions possibly leading
124 to different florigen-containing complexes are very high (Tylewicz et al., 2015; Park et al., 2014; Tsuji
125 et al., 2013; Li et al., 2015). Additionally, the floral transition in rice is associated with both induction
126 and repression of gene expression at the SAM, and different complexes could operate by promoting or
127 repressing expression of specific targets (Tamaki et al., 2015). Here, we demonstrate that canonical FACs
128 can also form in leaves where Hd3a and RFT1 interact through Gf14c with OsFD1. These complexes are
129 required to activate a positive feedback loop on *Ehd1*, *Hd3a* and *RFT1* expression. This function is
130 counterbalanced by two OsbZIP transcription factors closely related to OsFD1 that directly bind Hd3a
131 and function as negative regulators of the *Ehd1*-florigens module in leaves. Finally, we provide evidence
132 for a meristematic function of one such OsbZIP to repress the floral transition by reducing the expression
133 of inflorescence identity genes. We propose that dynamic formation of distinct complexes fine tunes
134 flowering in leaves and at the SAM of rice.

135

136 **RESULTS**

137 **An active florigen activation complex can form in leaves**

138 The rice (*Oryza sativa*) FAC is a transcriptional activation complex assembled in cells of the SAM by
139 Hd3a or RFT1, a Gf14 protein and OsFD1, and its primary targets include members of the *OsMADS*
140 transcription factor family (Kojima et al., 2002; Taoka et al., 2011; Tsuji et al., 2013; Tamaki et al., 2015;
141 Kobayashi et al., 2012). It has been proposed that FAC complexes control a wide range of developmental
142 processes in distinct tissues of several plant species, but to which extent a FAC might function outside
143 of the SAM and in rice leaf tissues is unclear. The diurnal mRNA expression of components of the FAC
144 was quantified under inductive and non-inductive photoperiods, including SD (10 h light) and LD (16 h
145 light) in the leaves (Supplemental Figure 1A-D). The expression of *Gf14c* did not depend upon the
146 photoperiod, and showed a peak at *Zeitgeber* (ZT) 15 (Supplemental Figure 1B). Expression of *OsFD1*
147 was detected under both photoperiods; however, its expression under LD was constant during the time
148 course, whereas it oscillated under SD with a peak in the middle of the night (Supplemental Figure 1C).
149 Similarly, expression of *Hd3a* and *RFT1* was induced during the night and peaked towards the end of it
150 (Supplemental Figure 1A).

151 Since all FAC components were co-expressed in leaves under SD, the expression of *OsMADS14* was
152 used as readout for the activity of the FAC. *OsMADS14* mRNA showed a peak during the night only in
153 leaves of plants grown under SDs, similarly to *OsFD1* (Supplemental Figure 1D). Additionally,
154 expression of both *OsMADS14* and *OsMADS15* was induced in leaves upon shifting plants from LD (16
155 h light) to SD (10 h light), as more Hd3a and RFT1 became available for FAC formation (Supplemental
156 Figure 1E-F). Expression of *OsMADS* TFs is therefore sensitive to expression of FAC components in
157 both leaves and meristem (Taoka et al., 2011; Kobayashi et al., 2012).

158 Based on relative transcript quantifications, *OsFD1* maximum expression was 5 times lower relative to
159 *Hd3a* or *RFT1* and about 50 times lower than *Gf14c* (compare y-axis scales in Supplemental Figure 1A-
160 C). Although relative mRNA amounts cannot be accurately compared between genes, these data
161 suggested that OsFD1 might be a limiting factor to FAC formation in leaves. To test this hypothesis, the
162 coding sequence (cds) of *OsFD1* was expressed under the constitutive rice *ACTIN2* promoter
163 (*proACT:OsFD1*) and expression of *OsMADS14* and *OsMADS15* was quantified at 6 and 13 days after
164 shifting plants from LD to SD (Figure 1A-C). In *proACT:OsFD1* plants, *OsMADS14* and *OsMADS15*
165 expression was strongly up-regulated in leaves at the indicated time points, compared to wild-type plants
166 grown under the same conditions, indicating that increasing OsFD1 abundance results in higher induction
167 of FAC target genes (Figure 1B,C).

168 Following the same rationale, we conditionally overexpressed *Hd3a* or *RFT1* in leaves under LD, when
169 *Gf14c* and *OsFD1*, but not *Hd3a* or *RFT1*, are expressed. To control overexpression, dexamethasone-
170 inducible (DEX) *Hd3a* or *RFT1* overexpressing plants were produced (*proGOS2:GVG 4xUAS:Hd3a* and
171 *proGOS2:GVG 4xUAS:RFT1*; hereafter referred to as *GVG:Hd3a* and *GVG:RFT1*, Figure 2A). We used
172 a previously validated system for inducible gene expression, composed of a DEX-inducible component
173 that drives expression of the genes of interest (Ouwkerk et al., 2001). Using this system, we avoided
174 the need for a chimeric florigen-glucocorticoid receptor protein, whose size might impinge on *Hd3a* or
175 *RFT1* protein movement or activity.

176 Transgenic plants containing *GVG:Hd3a* or *GVG:RFT1* could overexpress transgenic *Hd3a* or *RFT1*
177 only upon DEX treatments (Figure 2B,C). While a negligible basal expression of *OsMADS14* and
178 *OsMADS15* was observed in leaves of untreated plants under LD, expression of *OsMADS14* and
179 *OsMADS15* was strongly activated 16 hours after DEX treatment, concomitantly to *Hd3a* or *RFT1*
180 induction (Figure 2D,E).

181 Taken together, these experiments indicate that *OsMADS14* and *OsMADS15* transcription in leaves is
182 activated upon co-expression of all FAC components that are likely to form an active complex, as in the
183 SAM.

184

185 **A negative feedback loop independent of *OsFD1* limits florigen expression in leaves**

186 The expression of *Hd3a* and *RFT1* is transiently activated in leaves of plants grown under natural field
187 or artificial conditions. This observation suggests the existence of a mechanism that down-regulates their
188 expression upon commitment to flowering and that could possibly depend on *Ehd1*, encoding a common
189 upstream promoter of *Hd3a* and *RFT1* expression (Goretti et al., 2017; Ogiso-Tanaka et al., 2013;
190 Gómez-Ariza et al., 2015). Under our growing conditions, expression of the florigens reached a peak
191 about 12–15 days after shifting plants from LD to SD (Galbiati et al., 2016). We tested whether *Hd3a*
192 and *RFT1* are causal to their own down-regulation in leaves after the floral transition. The *GVG:Hd3a* or
193 *GVG:RFT1* transgenic plants were grown under LD (16 h light) and then shifted to SD (10 h light) to
194 induce expression of the endogenous *Hd3a* and *RFT1* transcripts in leaves. After 13 SD, half of the plants
195 were DEX-treated to overexpress transgenic *Hd3a* or *RFT1* (Figure 3A,C). Leaf samples were harvested
196 16 hours after DEX treatment at ZT0, when endogenous *Ehd1*, *Hd3a* and *RFT1* were highly expressed.
197 Quantification of transcripts indicated that the endogenous *Ehd1*, *Hd3a* and *RFT1* transcripts were
198 strongly downregulated in DEX-treated plants compared to mock-treated controls (Figure 3B,D). A
199 similar reduction of transcripts abundance was observed when either of the two florigens was induced

200 (Figure 3A-D). We tested several independent lines of both *GVG:Hd3a* and *GVG:RFT1* for DEX-
201 dependent control of *Ehd1*, *Hd3a* and *RFT1* transcripts. Despite a varying degree of inducibility among
202 independent transgenic lines, as quantified by the increase in *Hd3a* and *RFT1* expression in response to
203 DEX, we consistently observed reduction of endogenous *Ehd1*, *Hd3a* and *RFT1* transcripts
204 (Supplemental Figure 2 A,B). Therefore, both Hd3a and RFT1 can mediate a negative feedback loop on
205 *Ehd1* and, indirectly, on their own expression. The negative loop is activated also at low levels of
206 expression of transgenic *Hd3a* or *RFT1*, suggesting that it finely adjusts expression of the florigens
207 during floral induction.

208 A canonical OsFD-containing FAC could be required for negative regulation of *Hd3a* and *RFT1*
209 expression. Since OsFD1 is limiting to FAC formation in leaves at 12 DAS, expression of the florigens
210 was analyzed in *proACT:OsFD1* plants at this time point. Compared to wild type plants, constitutive
211 expression of *OsFD1* induced the up-regulation of *Hd3a*, *RFT1* and *Ehd1* expression (Figure 3E,F).
212 These data suggest that OsFD1 can promote expression of *Ehd1*, *Hd3a* and *RFT1* in leaves, and is not
213 part of the mechanism that self-limits expression of the florigens.

214

215 **Identification of FAC components expressed in leaves**

216 In rice and other plant species, many bZIP TFs have been already described that form alternative FACs
217 with the florigens, and control different developmental processes (Tylewicz et al., 2015; Tsuji et al.,
218 2013; Li et al., 2015). Whether other TFs abundant in leaves might form alternative FACs with a
219 flowering repressive function was evaluated. We performed untargeted and targeted yeast two-hybrid
220 screens using Hd3a and RFT1 as baits. Only the results of targeted screens will be presented in this study.
221 We selected members of the bZIP family of transcription factors based on sequence similarity with
222 OsFD1, wheat TaFDL2 (Li et al., 2015; Li and Dubcovsky, 2008) and maize DLF1 (Muszynski et al.,
223 2006) (Supplemental Figure 3A and Supplemental Data set 1), and we tested their interaction with Hd3a
224 and RFT1. Since it has been shown that bZIP TFs bind DNA by forming homo- and hetero-dimers, we
225 also tested their ability to homo- and hetero-dimerize. OsFD1 interaction with Gf14c was used as positive
226 control (Taoka et al., 2011). A summary of all interactions is reported in Table 1. We excluded from this
227 analysis *OsZIP29* as we could not amplify it from cDNA of LD- or SD-grown plants, *bZIP54/OsFD6*
228 as it is inferred to be a pseudogene (Tsuji et al., 2013), and finally genes whose interaction patterns have
229 already been determined (Tsuji et al., 2013). The *OsZIP24/OsFD3* and *OsZIP69/OsFD4* proteins could
230 not interact in our yeast assay with Hd3a or RFT1, although a recent report indicates weak interaction
231 with RFT1 (Jang et al., 2017). *OsZIP24/OsFD3* could interact with Gf14c while *OsZIP69/OsFD4*

232 could not. Conversely, OsbZIP62, OsbZIP42 and OsbZIP9 could interact with Hd3a but not with RFT1,
233 indicating some binding preference for one of the florigens. However, they also interacted with Gf14c,
234 which could possibly bridge the interaction with both florigens.

235 Among the bZIP TFs tested, we identified OsbZIP62, OsbZIP42 and OsbZIP9 as interactors of Hd3a and
236 Gf14c (Table 1 and Figure 4A). Based on their functional characterization, we renamed OsbZIP42 and
237 OsbZIP9 as Hd3a BINDING REPRESSOR FACTOR 1 (HBF1) and HBF2, respectively. The HBF1
238 and HBF2 proteins share 19.13% and 20.75% amino acid identity with OsFD1, and cluster in the same
239 branch of the bZIP phylogenetic tree (Supplemental Figure 3A). They share 68% identity with each other
240 when the full-length proteins are considered.

241 To further validate the direct interactions of HBF1, HBF2 and OsbZIP62 with Hd3a, Bimolecular
242 Fluorescent Complementation (BiFC) experiments were performed. The YFP N-terminus was fused to
243 each bZIP transcription factor creating HBF1-YFP N, HBF2-YFP N and bZIP62-YFP N chimeric
244 proteins, whereas the YFP C-terminus was fused to Hd3a (Hd3a-YFP C) (Figure 4B). Leaves of
245 *Nicotiana benthamiana* were infiltrated with Hd3a-YFP C and each of the bZIP chimeric fusions, and
246 nuclei of the epidermis showed strong YFP fluorescence, indicating physical interactions between Hd3a
247 and HBF1, HBF2 or bZIP62 as well as nuclear localization of the heterodimers. No fluorescence was
248 observed in nuclei co-expressing OsFD1-YFP N and Hd3a-YFP C, confirming the indirect interaction
249 between OsFD1 and Hd3a (Taoka et al., 2011).

250 Interactions were also assessed by Förster resonance energy transfer (FRET) fluorescence lifetime
251 imaging microscopy (FLIM) (Berezin and Achilefu, 2010). In FRET-FLIM measurements, the readout
252 for FRET is a reduced lifetime of the donor molecule in the FRET sample, compared to the donor-only
253 sample. FRET occurs when two molecules interact directly. A decrease in the Hd3a-GFP donor lifetime
254 was observed in the presence of HBF1-mCherry, HBF2-mCherry and OsbZIP62-mCherry, confirming
255 direct interactions in *Nicotiana benthamiana* epidermal nuclei (Figure 4C,D). No significant reduction
256 of donor lifetime was observed when co-expressing Hd3a-GFP and OsFD1-mCherry (Figure 4C,D).

257 Direct interactions between HBF1, HBF2 and Hd3a were conclusively assessed *in vitro* by GST-pull
258 down assays. We fused HBF1 and HBF2 to the Maltose Binding Protein (MBP) and incubated them with
259 either Gf14c-GST or Hd3a-GST immobilized on a glutathione resin. Both bZIPs bound Gf14c-GST and
260 Hd3a-GST, but not GST alone (Figure 4E and Supplemental Figure 3E). These data confirm that
261 interactions between HBF1, HBF2 and Hd3a occur in nuclei and do not require an intermediate 14-3-3
262 protein.

263 Finally, since bZIP TFs bind the DNA as dimers (Schütze et al., 2008; Reinke et al., 2013), we also tested
264 the possibility that HBF1 and HBF2 could heterodimerize with each other or with OsFD1. We did not
265 observe heterodimerization between these proteins in yeast (Table 1) or using the FRET-FLIM system
266 (data not shown), indicating that HBF1, HBF2 and OsFD1 are likely part of distinct transcriptional
267 complexes.

268 Diurnal time courses were used to determine the spatiotemporal expression of *OsZIP62*, *HBF1* and
269 *HBF2* (Supplemental Figure 3B-D). The mRNA expression of *OsZIP62* was most abundant in the SAM
270 under SD, and showed no strong oscillation during the 24 h cycle, despite a slight decline during the
271 night. Transcript abundance was negligible in leaves, indicating that *OsZIP62* is likely not part of a
272 complex limiting *Hd3a* expression in leaves but is possibly part of an Hd3a-containing complex in cells
273 of the SAM (Supplemental Figure 3D). Transcripts of *HBF1* and *HBF2* were highly expressed in the
274 SAM and showed expression also in leaves. *HBF1* transcription in leaves reached a peak during the night,
275 when *Hd3a* transcripts are also abundant (Supplemental Figure 3B-C). Taken together, these data
276 indicate that HBFs can potentially form distinct complexes both in the SAM and leaves.

277

278 ***HBF1* and *HBF2* encode floral repressors that reduce *Ehd1*, *Hd3a* and *RFT1* expression in leaves**

279 Whether *HBF1* and *HBF2* could influence flowering or expression of the florigens in leaves was assessed
280 by overexpressing them under the constitutive *ACT* promoter (Supplemental Figure 3F,G). Expression
281 of *Ehd1*, *Hd3a* and *RFT1* was monitored during photoperiodic induction of plants shifted from LD (16 h
282 light) to SD (10 h light). Leaves of the *proACT:HBF1* and *proACT:HBF2* plants showed a marked down-
283 regulation of *Ehd1*, *Hd3a* and *RFT1* expression compared to the wild type, unlike what observed in
284 *proACT:OsFD1* transgenic plants (Figure 5A,B). In agreement with the overall downregulation of the
285 *Ehd1*-florigens module, *proACT:HBF1* and *proACT:HBF2* plants flowered late when grown for 2
286 months under LD and then shifted to SD (Figure 5C).

287 We obtained the *hbfl-1* mutant from the PFG T-DNA collection in the cultivar Dongjin (Jeon et al.,
288 2000). Quantification of transcripts in the mutant showed that expression of *HBF1* was strongly reduced,
289 because of insertion of the T-DNA in the promoter (Supplemental Figure 4A,B). We analyzed the
290 flowering behavior of the *hbfl-1* mutant and observed that it headed earlier by ~5 days compared to
291 segregating wild-type siblings under continuous LD (14.5 h light) and by ~9 days under SD (10 h light)
292 (Figure 5D). To link the mutant phenotype with photoperiodic regulation of the *Ehd1*-florigen module,
293 transcript abundance of *Ehd1*, *Hd3a* and *RFT1* was determined at two time points after shifting plants
294 from LD to SD (10 and 17 DAS). The mRNA accumulation of all genes was higher in the *hbfl-1* mutant

295 compared to the wild type at both time points, indicating de-repression of the module (Figure 5E-G). To
296 exclude an indirect effect of HBF1 on *Ehd1* expression, the expression of six genes upstream of *Ehd1*
297 was also measured (Supplemental Figure 4C,D). None of them showed a difference in gene expression
298 between the wt and the *hbf1-1* mutant. The only exception was *Ghd7*, which was slightly downregulated
299 in the mutant compared to the wild type (Supplemental Figure 4D).

300 To confirm that loss of *HBF1* function promotes flowering and also to assess a possible functional
301 redundancy between *HBF1* and *HBF2*, we generated a series of double *hbf1 hbf2* mutants in the cultivar
302 Nipponbare, using the CRISPR/Cas9 technology (Miao et al., 2013). We designed a single guide-RNA
303 (sgRNA) on a region highly conserved between *HBF1* and *HBF2* on their first exon, to simultaneously
304 target both loci (Supplemental Figure 5A). Upon regeneration of transgenic plants, we obtained 6
305 independent lines harboring different combinations of biallelic or homozygous indels (Supplemental
306 Figure 5B). We selected five T2 lines (#1.2, #2.1, #4.1, #4.2, #6.1) from 4 independent T1s (#1, #2, #4,
307 #6), all of which were homozygous for *hbf1* mutations and homozygous or biallelic for *hbf2*
308 (Supplemental Figure 5C). All lines were double *hbf1hbf2* loss-of-function mutants, except line #4.1
309 which contained a homozygous -27 bp in-frame deletion at the *HBF1* locus, likely not causing loss of
310 gene function (Supplemental Figure 5C). We measured their flowering time under LD (14.5 h light) and
311 after growth for 8 weeks under LD followed by SD (10 h light). Under both conditions, all *hbf1 hbf2*
312 double loss-of-function mutants flowered earlier compared to the wild type (Figure 5H-K), but flowering
313 was not accelerated in line #4.1. These data indicate that loss of 9 amino acids (EDFLVKAGV before
314 the bZIP domain) in the HBF1 protein likely does not affect its function. They further indicate that the
315 *hbf2* mutation does not additively contribute to the phenotype caused by single *hbf1* mutations. As
316 opposed to the effect of the *hbf1-1* allele in Dongjin, the Nipponbare *hbf1 hbf2* CRISPR mutants showed
317 predominantly accelerated flowering under LD (~13 days was the largest difference observed between
318 line #1.2 and the WT), rather than under SD (the same line #1.2 flowered ~5 days earlier than the WT).
319 We attribute these differences to the different sensitivity of Dongjin and Nipponbare to loss of HBF1
320 function.

321

322 **HBF1 can bind the *Ehd1* promoter**

323 Expression of *Ehd1* is dependent upon HBF1 activity. The *Ehd1* promoter region was scanned in search
324 of conserved motifs recognized by bZIP TFs, and we found 3 CACGTC motifs that are characteristic of
325 Abscisic Acid Response Elements (ABRE) and G-boxes (Li and Dubcovsky, 2008) (Supplemental
326 Figure 5D). As expected by the central position of *Ehd1* in flowering regulatory networks, many other

327 motifs were identified in its promoter region spanning 1.5 kb upstream of the ATG (Supplemental Figure
328 5D). The possibility of a direct interaction between HBF1 and the *Ehd1* promoter was assessed using
329 Electrophoretic Mobility Shift Assay (EMSA). The HBF1 protein was purified and incubated with a
330 Cy5-labelled oligonucleotide identical to the region of the *Ehd1* promoter containing the ABRE, located
331 at -482 bp (Supplemental Figure 5D). HBF1 binding to this oligonucleotide resulted in a band shift
332 (Figure 6D). Addition of an excess of unlabeled oligonucleotide reversed the shift of the fluorescent
333 probe. However, no band shift could be detected when HBF1 was incubated with a promoter fragment
334 containing a CArG-box, demonstrating that HBF1 binding to the ABRE-containing region was specific
335 (Figure 6D). No ABREs or G-boxes were identified by scanning the *Hd3a* or *RFT1* promoters, although
336 indirect binding of HBF1 to these genes cannot be completely excluded.

337

338 **HBF1 represses transcription of *OsMADS14* and *OsMADS15* in the shoot apical meristem**

339 The *HBF1* and *HBF2* transcripts could be identified in both leaves and SAMs, suggesting that they are
340 expressed in both florigen-producing and -receiving tissues. Their overexpression delayed flowering, and
341 in leaves it reduced mRNA expression of *Hd3a* and *RFT1*. Whether these proteins also had a role in the
342 SAM to control flowering or gene expression was tested by misexpression studies. To this end, the
343 promoter of *ORYZA SATIVA HOMEBOX 1* (*proOSH1*) was cloned and used to drive expression of
344 *HBF1*. *OSH1* is expressed in undifferentiated cells of the SAM but not in organ primordia arising from
345 it (Itoh et al., 2000; Sentoku et al., 1999). Transgenic *proOSH1:HBF1* rice plants that overexpressed
346 *HBF1* were produced. Transcriptional analysis of leaves and SAMs of T2 lines indicated that expression
347 driven by the *OSH1* promoter was effective at increasing expression of *HBF1* at the SAM but not in
348 leaves (Figure 6A). The same plants had delayed flowering by few days compared to non-transgenic
349 segregating controls (Figure 6B). Our dissection of SAMs included also some of the youngest leaf
350 primordia arising from the meristem; however, the *OSH1* promoter is not active in this tissue (Tsuda et
351 al., 2011). Thus, we conclude that the flowering delay is caused by increased expression of *HBF1* in
352 meristematic cells. Transcripts of *Hd3a* and *RFT1* were not expressed at the meristem; therefore,
353 although we cannot fully exclude the expression of other *FT*-like genes, feedback regulation of these
354 florigens is likely not occurring at the apex.

355 Finally, the expression of *OsMADS14* and *OsMADS15* was found to be significantly reduced in SAMs
356 (Figure 6C). These data indicate that *HBF1* at least, can repress flowering and expression of inflorescence
357 identity genes at the SAM, and therefore has a dual transcriptional repressive function in distinct plant
358 compartments.

359

360 **Discussion**

361 Dexamethasone treatment of plants expressing inducible versions of *Hd3a* and *RFT1* indicated the
362 existence of transcriptional repression of the florigens mediated by a feedback negative loop.

363 Thus, we propose a modification of the rice (*Oryza sativa*) floral induction model to include an auto-
364 regulatory loop centered on *Hd3a* and *RFT1*. The florigens regulate their own expression in leaves by
365 forming distinct FACs with several OsbZIP proteins (Figure 7). These complexes can either promote or
366 repress *Ehd1*, *Hd3a* and *RFT1* depending on the interacting bZIP. In particular, OsFD1 acts as
367 transcriptional activator in leaves, whereas the closely related HBFs repress expression of the florigens
368 in the same tissue. Thus, Hd3a and RFT1 proteins can engage into both florigen activation and repression
369 complexes. Binding of HBF1 to the promoter of *Ehd1* further provides molecular evidence for feedback
370 regulation of the florigens. The preference of RFT1 and Hd3a to interact with OsFD1 or the HBFs can
371 be driven by relative expression patterns or modifications of OsFD1 and the HBFs under different
372 growing conditions. Both the *HBF1* and *HBF2* transcripts are expressed in the SAM as well, and tissue-
373 specific overexpression of *HBF1* at least, could reduce the expression of targets of the FAC at the apex.
374 These data identify a previously unknown function for the rice florigens in leaves, and suggests the
375 existence of a regulatory layer limiting Hd3a and RFT1 signaling to fine tune production of the florigens
376 in leaves and their effect on gene regulatory networks at the apical meristem.

377

378 **The rice florigens act in leaves to regulate their own expression**

379 A growing number of studies demonstrate that FT-like proteins are involved in a wide range of
380 developmental processes, including tuberization (Navarro et al., 2011), bulbing (Lee et al., 2013),
381 stomatal opening (Kinoshita et al., 2011), leaf curling (Teper-Bamnlker and Samach, 2005), vegetative
382 growth in trees (Hsu et al., 2011), plant architecture in tomato (Park et al., 2014), and tillering in rice
383 (Tsuji et al., 2015). In many such instances, they function in tissues different from the SAM. However,
384 FT-like proteins have been most prominently described in the context of flowering time control in
385 response to environmental cues. During this process, they act as long distance flowering promoters
386 produced in leaves and translocated to the SAM, inducing developmental switches upon the formation
387 of a FAC (Lifschitz et al., 2006; Corbesier et al., 2007; Mathieu et al., 2007; Tamaki et al., 2007). The
388 data presented in this study suggest that a FAC can form also in rice leaves to activate expression of the
389 same targets normally transcribed in the SAM. That a FAC is active also in leaves was initially suggested
390 by experiments in *Arabidopsis* (Teper-Bamnlker and Samach, 2005). Expression of *FT* or *Tomato FT*

391 (*TFT*) in transgenic *Arabidopsis* plants from the viral 35S promoter caused leaf curling that could be
392 suppressed by mutating *FD*, *SEP3* or *FUL*. These data indicated that a FAC formed in leaves under
393 specific conditions could perturb leaf development by promoting transcription of targets usually
394 expressed at the SAM (Teper-Bamnolker and Samach, 2005).

395 Whether a FAC has any biologically relevant function in leaves of *Arabidopsis* remains to be clarified.
396 However, the identification of *Ehd1*, *Hd3a* and *RFT1* as targets of florigen-containing complexes in
397 leaves of rice suggests that one function of these complexes is feed-back tuning of the expression of some
398 of its own components. In particular, by reducing transcription of *Ehd1*, florigen repressor complexes
399 can indirectly limit expression of *Hd3a* and *RFT1*, downstream targets of *Ehd1* (Doi et al., 2004; Zhao
400 et al., 2015). Since seasonal expression of the rice florigens is transient and is strongly reduced upon
401 completion of the floral transition, a plausible biological role for this auto-regulatory loop could be to
402 switch off transcription of the florigens upon floral commitment. Alternatively (or in parallel), it could
403 fine tune the production of Hd3a and RFT1 during photoperiodic induction (Gómez-Ariza et al., 2015;
404 Ogiso-Tanaka et al., 2013). More data will be required to distinguish between these possibilities and
405 validate them but it is clear that reproductive commitment requires a tight balance between flowering
406 promoting and repressive complexes, whose equilibrium could be controlled by modulating the
407 expression levels of distinct bZIPs by developmental or environmental factors (Tang et al., 2016; Wu et
408 al., 2014; Zhang et al., 2016), or by controlling their activity through phosphorylation (Kagaya et al.,
409 2002; Choi et al., 2005; Furihata et al., 2006). Indeed, phosphorylation of OsFD transcription factors is
410 required for binding to 14-3-3 proteins and is limiting to FAC function (Taoka et al., 2011).

411 Auto-regulatory motifs are likely very common in gene regulatory networks, but can be identified and
412 studied only by quantifying endogenous transcripts in plants expressing transgenic copies of the same
413 gene or its closely related homologues. Such approach has led to the identification of a loop regulating
414 *StSP6A* expression, encoding a tuberigen, the mobile protein causing tuber formation at the apical
415 meristem of potato stolons, and sharing high sequence similarity with *Hd3a* (Navarro et al., 2011). A
416 similar auto-regulatory loop in the expression of an endogenous florigen has been recently reported in
417 *Chrysanthemum*, where transcriptional induction of *CsFTL3* required a complex formed by *CsFTL3* and
418 *CsFDL1* proteins (Higuchi et al., 2013). It is noteworthy that regulatory loops involving two FT-like
419 proteins are also very common among Angiosperms. The FT-like SP5G proteins of potato and tomato
420 inhibit expression of the *SINGLE FLOWER TRUSS* (*SFT*) florigen and of *StSP6A*, respectively
421 (Abelenda et al., 2016; Soyk et al., 2016). Similar modules in which an FT-like protein inhibits
422 developmental transitions by repressing a second FT-like gene have been reported also for flowering in

423 sugar beet (Pin et al., 2010; Higuchi et al., 2013) and bulbing in onion (Lee et al., 2013). In rice, both
424 auto-regulatory and relay mechanisms between Hd3a and RFT1 are possible under inductive conditions,
425 when both proteins are expressed. Their differential ability to directly bind to HBFs might underlie
426 differences in their capacity to take part in positive or negative relay mechanisms, but this type of cross
427 regulation is difficult to dissect genetically, because of the redundancy between these factors. However,
428 in general, auto-regulatory and relay mechanisms among florigen-like proteins are emerging as very
429 common modules controlling developmental switches.

430

431 **Florigen-containing complexes exhibit combinatorial properties**

432 Florigen activation complexes from several species have a modular structure where distinct bZIP proteins
433 can interact with different FT-like proteins in a combinatorial fashion (Susmilch et al., 2015; Tsuji et
434 al., 2013). Temporal and spatial dynamics of complex formation highly expand the regulatory
435 possibilities of such complexes to control plant development. In rice leaves, Hd3a and RFT1 can form
436 complexes displaying transcriptional promoting or repressive activity depending on the interacting bZIP.
437 Since HBF1, HBF2 and OsFD1 do not heterodimerize, they cannot be part of the same complex, in
438 agreement with their opposite functions. Additionally, since HBF1 and HBF2 do not interact with each
439 other, they are possibly part of independent complexes.

440 Different examples in plants suggest that the functional specificity of these regulatory complexes can be
441 provided by the bZIP as well as the FT-like protein. In rice, branching of shoots and altered panicle
442 architecture are induced upon overexpression of OsFD2 (Tsuji et al., 2013). This bZIP can interact with
443 Hd3a, and the interaction is bridged by the Gf14b protein. Given that OsFD2 controls patterns of
444 vegetative growth, it could be speculated that FACs are active during distinct phases of the plant life
445 cycle and not only during reproduction. Additionally, it raises the interesting possibility that complexes
446 dynamically changing the Gf14 protein component might take on different roles. However, functional
447 studies with Gf14 mutants are complicated by their pleiotropy and essential nature (Purwestri et al.,
448 2009).

449 In hybrid aspen, overexpression of FDL1 but not FDL2 delays bud set and growth cessation, indicating
450 FDL1 specificity for these developmental processes. However, both FDLs could interact with FT1 and
451 FT2 to activate downstream targets in transient heterologous systems (Tylewicz et al., 2015). In these
452 examples, specificity is likely contributed by the FD-like transcription factor.

453 Conversely, distinct PEBP components binding to the same bZIP protein can switch its function.
454 Arabidopsis FD can interact with FT but also with TFL1, to form a flowering repressive complex

455 (Hanano and Goto, 2011; Ho and Weigel, 2014). Similar interaction patterns are also possible in tomato
456 between SP3G/SPP, an FD homolog, and the TFL1-like protein SELF PRUNING (SP) or the SFT
457 florigen, where the balance between complexes regulates shoot architecture and, ultimately, yield (Pnueli
458 et al., 2001; Park et al., 2014). Finally, the floral transition in Arabidopsis axillary meristems is controlled
459 by the TCP transcription factor BRANCHED1, directly interacting with the PEBPs FT and TWIN
460 SISTER OF FT (TSF) but not with TFL1 (Niwa et al., 2013). Overall, these patterns indicate that a basal
461 conserved module can be repurposed in distantly related species to control several developmental
462 programs, and that plasticity in complex assembly determines the balance between developmental
463 programs.

464

465 **Methods**

466 **Plant materials**

467 The *hbf1-1* mutant corresponds to the Salk line PFG_2D-00885 in the cultivar Donjing. Homozygous T-
468 DNA insertional mutants were selected using primers listed in Supplemental Table 1. The cultivar
469 Nipponbare was used in all other experiments.

470

471 **Growth conditions, sampling and quantification of gene expression**

472 Plants (*Oryza sativa*) were grown under LD (14.5 h light/9.5 h dark or 16 h light/8 h dark) or SD
473 conditions (10 h light/14 h dark) in Conviron PGR15 growth chambers. Light was provided by T8
474 fluorescent and halogen incandescent lamps. Light intensity was adjusted to level 3 for both sets of lamps,
475 resulting in $\sim 450 \mu\text{mol}/\text{m}^2/\text{s}$. Plant material was collected from the distal part of mature leaves, from at
476 least three plants/time point, at ZT0. Only for the experiments described in Figure 5E-G and in
477 Supplemental Figure 4C-D, plants were sampled at ZT20 under SD, as this time point corresponds to
478 peak expression of *Ehd1*. Only for the data described in Figure 5A and 5B, all samples were quantified
479 in the same experiments and then split into separate graphs for clarity of presentation. For SAM sampling,
480 at least five apices/sample were manually dissected under a stereomicroscope using scalpels. Sample
481 included the meristem, the two younger leaf primordia arising from it, as well as part of the rib meristem.
482 RNA was extracted from leaves using the TRIzol® reagent (Thermofisher Scientific), and from SAMs
483 using the NucleoSpin® RNA Plant kit (Macherey-Nagel). To prepare and quantify cDNAs, the RNA
484 was retro-transcribed using the ImProm-II reverse transcriptase (Promega), and the Maxima SYBR qPCR
485 master mix (Termofisher Scientific) was used to measure gene expression in a Mastercycler Real Plex²
486 (Eppendorf). All primers used in RT-qPCR experiments have an annealing temperature of 60°C. For

487 quantification of transcripts of *Hd3a* and *RFT1* endogenous mRNAs, *Ehd1*, *OsMADS14*, *OsMADS15*
488 and *UBQ*, we used primers described in Galbiati et al., 2016, and Gomez-Ariza et al., 2015. All other
489 primers used in this study are listed in Supplemental Table 1.

490

491 **Construction of transgenic plants and DEX treatments**

492 The *OsZIP* coding sequences were amplified from leaf or SAM cDNAs using primers listed in
493 Supplemental Table 1, and subsequently cloned in pDONR207 (Invitrogen). Plant expression vectors
494 were obtained by Gateway® cloning, recombining the cds after the *ACTIN* promoter in the pH2GW7
495 plasmid. The *Hd3a* and *RFT1* cds were amplified from leaves of Nipponbare with primers Os1-Os2,
496 Os3-Os2, respectively. The *pINDEX2* vector was used for DEX-inducible expression of *Hd3a* and *RFT1*
497 (Ouwerkerk et al., 2001), but it was first turned into a Gateway®-compatible (Invitrogen) destination
498 vector by blunt cutting with PmlI and insertion of an EcoRV-digested Gateway RFC cassette. A
499 *proOSHI:Gateway* destination construct was generated cloning a 1.5Kb promoter fragment using
500 primers Os_6 and Os_7 (Supplemental Table 1). The *pINDEX4* vector and *proOSHI* were then cut using
501 MunI and MluI and ligated to create *pINDEX4 proOSHI*. The RFA gateway cassette was inserted into
502 the *proOSHI pINDEX4* vector after blunt cutting using EcorV and StuI. Subsequently, the DEX
503 inducible cassette was removed by blunt cutting using SwaI and BbrPI and self-ligation of the vector.
504 The *proOSHI:HBFI* vector was generated by LR recombination (Invitrogen).

505 For rice transformation, embryogenic calli were produced from Nipponbare seeds, prepared and
506 transformed according to the protocol of Sahoo et al., 2011, using the EHA105 strain of *A. tumefaciens*.
507 Transgenic plants were selected on 50 mg/L and 100 mg/L hygromycin during selection I and II,
508 respectively. Gene expression of *Hd3a* and *RFT1* was induced by leaf-spray with 10 µm DEX solution
509 + 0.2% Tween, in transgenic homozygous T3 plants. DEX treatments were performed at ZT8 and
510 sampling was done 16 h later at ZT0. Induction efficiency was assessed by RT-qPCR on leaves using
511 primers specific for the *Hd3a* or *RFT1* coding sequences.

512

513 **Protein–protein interaction studies**

514 For yeast-2-hybrid studies, the coding sequences were cloned into the vectors pGADT7 and pGBKT7
515 (Clontech) Gateway® (Invitrogen) and transformed into AH109 and Y187 yeast strains, respectively.
516 Interactions were tested by mating and growth of diploid yeast on selective -L-W-H medium
517 supplemented with 3-aminotriazole (3AT). BiFC experiments were performed in *Nicotiana benthamiana*
518 epidermal cells with the vectors pBAT TL-B sYFP-N and pBAT TL-B sYFP-C. FRET-FLIM

519 experiments were performed in *N. benthamiana* epidermal cells transformed with the β -estradiol
520 inducible vectors pABIND-GFP and pABIND-mCherry (Bleckmann et al., 2010; Somssich et al., 2015).
521 β -estradiol induction of the transgenes was performed with 20 μ M β -estradiol and 0.1 % Tween20 4-6
522 hours before measurements. FRET-FLIM measurements were performed on 10 co-transformed nuclei at
523 least and mean, standard deviation and p-value (Student's t test) of the donor lifetime for the various sets
524 of experiments was calculated, as described by Stahl et al., 2013.

525

526 **GST-pull down**

527 The GST-Hd3a and GTS-GF14c fusion proteins were obtained by recombining the cds into pDEST15
528 (Invitrogen), expressing them using BL21 (DE3) cells (Invitrogen) and purifying them with Glutathione
529 Sepharose 4b® (Sigma). The concentration of each fusion protein was determined using Bradford assays.
530 Equal amounts of GST-fusion proteins and GST were incubated in TIF buffer (150 mM NaCl, 20 mM
531 Tris pH 8.0, 1 mM MgCl₂, 0.1% NP40, 10% glycerol) and added to 2 ml of clarified bacterial lysate of
532 BL21 (DE3) cells expressing HBF1 and HBF2 proteins fused to MBP (pMAL vector adapted to Gateway
533 system). The bacterial lysate was obtained by sonication of a bacterial pellet resuspended in TIF buffer
534 supplemented with cOmplete Protease Inhibitor Cocktail® (Roche). The reaction mixture was incubated
535 for 2 h at 4°C under gentle rotation. After three washes with TIF buffer and 2 washes with PBS buffer,
536 the resins were resuspended with SDS-PAGE loading buffer and eluted at 99°C for 5 min. The eluted
537 proteins were resolved in 10% SDS-PAGE and immunoblot analysis was performed using a monoclonal
538 anti-MBP HRP-conjugated antibody (BioLabs).

539

540 **Phylogenetic analysis**

541 Sequences of bZIP proteins were retrieved from public databases and aligned using the CLC Genomics
542 Workbench program with the following parameters: Gap open cost = 20.0; Gap extension cost = 10.0
543 End gap cost = As any other; Alignment mode = Very accurate. An unrooted phylogenetic tree was
544 created on the alignment using the Neighbor Joining algorithm. Distances were measured using the
545 Jukes-Cantor model. Bootstrap values are indicated at each node based on 1000 replicates. Sequence
546 alignments are reported in Supplemental Data Set 1.

547

548 **CRISPR-Cas9 editing**

549 The CRISPR-Cas9 vector was previously described (Miao et al., 2013). The sgRNA oligo (Os_934)
550 targeting both *HBF1* and *HBF2* was designed based on the first exon of both genes, upstream of the

551 region encoding the bZIP domain and expressed in transgenic Nipponbare. Transformation was
552 performed as described above. The *HBF1* and *HBF2* loci in the regenerating plants were amplified and
553 sequenced using primers Os_551-Os_338 and Os_976-Os_553 respectively, to identify the mutations
554 introduced by non-homologous end joining. The same primers were used to genotype the subsequent
555 plant generations.

556

557 **Electromobility shift Assays**

558 Consensus sequences in the *Ehd1* promoter (1.5 kb upstream of the ATG) were identified using the Nsite
559 software (Shahmuradov and Solovyev, 2014). The sequences of the ABRE and CArG-box containing
560 primers are shown in Supplemental Table 1. The HBF1 protein fused to Maltose Binding Protein (MBP)
561 was expressed in the *E. coli* Rosetta strain and purified to homogeneity by passing it through a maltose
562 column followed by an ion exchange step (MonoQ). Binding of HBF1 to the *Ehd1* promoter was tested
563 using 25 pmol of Cy5-labeled DNA duplexes (either ABRE or CArG-box sequences, Supplemental
564 Table 1) mixed with 150 pmol of the purified protein in 20 mM trisHCl, pH 8.0, 200 mM NaCl. In the
565 competition studies, the mixture was supplemented with increasing amounts (1:2 to 1:25 molar ratio) of
566 unlabeled DNA. Precast Novex TBE gels (Thermofisher Scientific) were used for the electrophoretic
567 run.

568

569 **Accession Numbers**

570 Sequence data from this article can be found in the Rice MSU Genome Annotation Release 7 under the
571 following accession numbers: LOC_Os06g06320.1 (Hd3a), LOC_Os06g06300 (RFT1),
572 LOC_Os08g33370 (Gf14c), LOC_Os09g36910 (OsFD1), LOC_05g41070 (HBF1), LOC_Os01g59760
573 (HBF2), LOC_07g48660 (bZIP62), LOC_Os06g16370.1 (Hd1), LOC_Os10g32600.1 (Ehd1),
574 LOC_Os07g15770.1 (Ghd7), LOC_Os07g49460.1 (PRR37), LOC_Os03g54160.1 (OsMADS14),
575 LOC_Os07g01820.1 (OsMADS15).

576 **Supplemental Data**

577 **Supplemental Figure 1. Expression of FAC components and FAC targets in leaves.**

578

579 **Supplemental Figure 2. Independent Hd3a or RFT1 DEX-inducible transgenic lines show a range**
580 **of Hd3a or RFT1 DEX-dependent induction and downregulation of Ehd1, Hd3a and RFT1**
581 **endogenous expression.**

582

583 **Supplemental Figure 3. Selection of bZIP transcription factors putatively forming a**
584 **transcriptional complex with the florigens.**

585

586 **Supplemental Figure 4. Analysis of the *hbfl-1* mutant.**

587

588 **Supplemental Figure 5. Analysis of *hbfl hbfl2* CRISPR mutants and of the *HBFL1* promoter.**

589

590 **Supplemental Table 1. Primers used in this study.**

591

592 **Supplemental Data set 1.** Text file of the alignment used for the phylogenetic analysis shown in
593 Supplemental Figure 3A.

594

595 **Supplemental File 1.** Anova tables.

596

597 **Author Contributions**

598 V.B., Rü.S. and F.F. designed the research. V.B., D.M., D.G., M.S., M.d.R., M.C, F.G, R.S., F.L.
599 performed research. V.B and F.F. wrote the paper.

600

601 **Acknowledgments**

602 We thank Ludovico Dreni for providing the *proACTIN* overexpression vector, and Jin Miao and Li-Jia
603 Qu for providing the rice CRISPR-Cas9 vectors. This work was supported by an ERC Starting Grant
604 (#260963) to FF. The authors declare no conflict of interest.

605

606 **References**

- 607 **Abelenda, J., Cruz-Oró, E., Franco-Zorrilla, J., and Prat, S.** (2016). Potato StCONSTANS-like1
608 Suppresses Storage Organ Formation by Directly Activating the FT-like StSP5G Repressor. *Curr.*
609 *Biol.* **26**: 872–881.
- 610 **Andrés, F. and Coupland, G.** (2012). The genetic basis of flowering responses to seasonal cues. *Nat.*
611 *Rev. Genet.* **13**: 627–39.
- 612 **Berezin, M.Y. and Achilefu, S.** (2010). Fluorescence Lifetime Measurements and Biological Imaging.
613 *Chem. Rev.* (Washington, DC, U. S.) **110**: 2641–2684.
- 614 **Bleckmann, A., Weidtkamp-Peters, S., Seidel, C. a M., and Simon, R.** (2010). Stem cell signaling

615 in Arabidopsis requires CRN to localize CLV2 to the plasma membrane. *Plant Physiol.* **152**: 166–
616 76.

617 **Brambilla, V. and Fornara, F.** (2013). Molecular control of flowering in response to day length in
618 rice. *J. Integr. Plant Biol.* **55**: 410–8.

619 **Cho, L.-H., Yoon, J., Pasriga, R., and An, G.** (2016). Homodimerization of Ehd1 is required to
620 induce flowering in rice. *Plant Physiol.* **170**: pp.01723.2015.

621 **Choi, H., Park, H.-J., Park, J.H., Kim, S., Im, M.-Y., Seo, H.-H., Kim, Y.-W., Hwang, I., and
622 Kim, S.Y.** (2005). Arabidopsis calcium-dependent protein kinase AtCPK32 interacts with ABF4,
623 a transcriptional regulator of abscisic acid-responsive gene expression, and modulates its activity.
624 *Plant Physiol.* **139**: 1750–1761.

625 **Corbesier, L., Vincent, C., Jang, S., Fornara, F., Fan, Q., Searle, I., Giakountis, A., Farrona, S.,
626 Gissot, L., Turnbull, C., and Coupland, G.** (2007). FT Protein Movement Contributes to Long-
627 Distance Signaling in Floral Induction of Arabidopsis. *Science* **316**: 1030–1033.

628 **Danilevskaya, O.N., Meng, X., Hou, Z., Ananiev, E. V., and Simmons, C.R.** (2008). A Genomic
629 and Expression Compendium of the Expanded PEBP Gene Family from Maize. *Plant Physiol.*
630 **146**: 250–264.

631 **Doi, K., Izawa, T., Fuse, T., Yamanouchi, U., Kubo, T., Shimatani, Z., Yano, M., and Yoshimura,
632 A.** (2004). Ehd1, a B-type response regulator in rice, confers short-day promotion of flowering
633 and controls FT-like gene expression independently of Hd1. *Genes Dev.* **18**: 926–36.

634 **Furihata, T., Maruyama, K., Fujita, Y., Umezawa, T., Yoshida, R., Shinozaki, K., and
635 Yamaguchi-Shinozaki, K.** (2006). Abscisic acid-dependent multisite phosphorylation regulates
636 the activity of a transcription activator AREB1. *Proc Natl Acad Sci U S A* **103**: 1988–1993.

637 **Galbiati, F., Chiozzotto, R., Locatelli, F., Spada, A., Genga, A., and Fornara, F.** (2016). Hd3a ,
638 RFT1 and Ehd1 integrate photoperiodic and drought stress signals to delay the floral transition in
639 rice. *Plant. Cell Environ.* **39**: 1982–1993.

640 **Gómez-Ariza, J., Galbiati, F., Goretta, D., Brambilla, V., Shrestha, R., Pappolla, A., Courtois, B.,
641 and Fornara, F.** (2015). Loss of floral repressor function adapts rice to higher latitudes in Europe.
642 *J. Exp. Bot.* **66**: 2027–39.

643 **Goretta, D., Martignago, D., Landini, M., Brambilla, V., Gomez-Ariza, J., Gnesutta, N., Galbiati,
644 F., Collani, S., Takagi, H., Terauchi, R., Mantovani, R., and Fornara, F.** (2017).
645 Transcriptional and post-transcriptional mechanisms limit Heading Date 1 (Hd1) function to adapt
646 rice to high latitudes. *PLoS Genet.* **13**: e1006530.

647 **Hanano, S. and Goto, K.** (2011). Arabidopsis TERMINAL FLOWER1 is involved in the regulation of
648 flowering time and inflorescence development through transcriptional repression. *Plant Cell* **23**:
649 3172–84.

650 **Higuchi, Y., Narumi, T., Oda, A., Nakano, Y., Sumitomo, K., Fukai, S., and Hisamatsu, T.** (2013).
651 The gated induction system of a systemic floral inhibitor, antiflorigen, determines obligate short-
652 day flowering in chrysanthemums. *Proc. Natl. Acad. Sci.* **110**: 17137–17142.

653 **Ho, W.W.H. and Weigel, D.** (2014). Structural features determining flower-promoting activity of
654 Arabidopsis FLOWERING LOCUS T. *Plant Cell* **26**: 552–64.

655 **Hsu, C.-Y. et al.** (2011). FLOWERING LOCUS T duplication coordinates reproductive and vegetative
656 growth in perennial poplar. *Proc. Natl. Acad. Sci. U. S. A.* **108**: 10756–61.

657 **Itoh, J.I., Kitano, H., Matsuoka, M., and Nagato, Y.** (2000). Shoot organization genes regulate shoot
658 apical meristem organization and the pattern of leaf primordium initiation in rice. *Plant Cell* **12**:
659 2161–74.

660 **Izawa, T., Foster, R., and Chua, N.H.** (1993). Plant bZIP protein DNA binding specificity. *J. Mol.*
661 *Biol.* **230**: 1131–1144.

662 **Jang, S., Choi, S.C., Li, H.Y., An, G., and Schmelzer, E.** (2015). Functional characterization of
663 phalaenopsis aphrodite flowering genes PaFT1 and PaFD. *PLoS One* **10**.

664 **Jang, S., Li, H.-Y., and Kuo, M.-L.** (2017). Ectopic expression of Arabidopsis FD and FD
665 PARALOGUE in rice results in dwarfism with size reduction of spikelets. *Sci. Rep.* **7**: 44477.

666 **Jaudal, M., Zhang, L., Che, C., and Putterill, J.** (2015). Three Medicago MtFUL genes have distinct
667 and overlapping expression patterns during vegetative and reproductive development and
668 35S:MtFULb accelerates flowering and causes a terminal flower phenotype in Arabidopsis. *Front.*
669 *Genet.* **6**: 50.

670 **Jeon, J.S. et al.** (2000). T-DNA insertional mutagenesis for functional genomics in rice. *Plant J.* **22**:
671 561–570.

672 **Kagaya, Y., Hobo, T., Murata, M., Ban, A., and Hattori, T.** (2002). Abscisic acid-induced
673 transcription is mediated by phosphorylation of an abscisic acid response element binding factor,
674 TRAB1. *Plant Cell* **14**: 3177–89.

675 **Kinoshita, T., Ono, N., Hayashi, Y., Morimoto, S., Nakamura, S., Soda, M., Kato, Y., Ohnishi,**
676 **M., Nakano, T., Inoue, S.I., and Shimazaki, K.I.** (2011). FLOWERING LOCUS T regulates
677 stomatal opening. *Curr. Biol.* **21**: 1232–1238.

678 **Kobayashi, K., Yasuno, N., Sato, Y., Yoda, M., Yamazaki, R., Kimizu, M., Yoshida, H.,**

679 **Nagamura, Y., and Kyojuka, J.** (2012). Inflorescence Meristem Identity in Rice Is Specified by
680 Overlapping Functions of Three AP1/FUL-Like MADS Box Genes and PAP2, a SEPALLATA
681 MADS Box Gene. *Plant Cell* **24**: 1848–1859.

682 **Kojima, S., Takahashi, Y., Kobayashi, Y., Monna, L., Sasaki, T., Araki, T., and Yano, M.** (2002).
683 Hd3a, a rice ortholog of the Arabidopsis FT gene, promotes transition to flowering downstream of
684 Hd1 under short-day conditions. *Plant Cell Physiol.* **43**: 1096–105.

685 **Komiya, R., Ikegami, A., Tamaki, S., Yokoi, S., and Shimamoto, K.** (2008). Hd3a and RFT1 are
686 essential for flowering in rice. *Development* **135**: 767–774.

687 **Komiya, R., Yokoi, S., and Shimamoto, K.** (2009). A gene network for long-day flowering activates
688 RFT1 encoding a mobile flowering signal in rice. *Development* **136**: 3443–3450.

689 **Lee, R., Baldwin, S., Kenel, F., McCallum, J., and Macknight, R.** (2013). FLOWERING LOCUS T
690 genes control onion bulb formation and flowering. *Nat. Commun.* **4**: 2884.

691 **Li, C. and Dubcovsky, J.** (2008). Wheat FT protein regulates VRN1 transcription through interactions
692 with FDL2. *Plant J.* **55**: 543–554.

693 **Li, C., Lin, H., and Dubcovsky, J.** (2015). Factorial combinations of protein interactions generate a
694 multiplicity of florigen activation complexes in wheat and barley. *Plant J.* **84**: 70–82.

695 **Lifschitz, E., Eviatar, T., Rozman, A., Shalit, A., Goldshmidt, A., Amsellem, Z., Alvarez, J.P., and**
696 **Eshed, Y.** (2006). The tomato *FT* ortholog triggers systemic signals that regulate growth and
697 flowering and substitute for diverse environmental stimuli. *Proc Natl Acad Sci U S A* **103**: 6398–
698 6403.

699 **Litt, A. and Irish, V.F.** (2003). Duplication and Diversification in the APETALA1/FRUITFULL
700 Floral Homeotic Gene Lineage: Implications for the Evolution of Floral Development. *Genetics*
701 **165**: 821–833.

702 **Mathieu, J., Warthmann, N., Küttner, F., and Schmid, M.** (2007). Export of FT protein from
703 phloem companion cells is sufficient for floral induction in Arabidopsis. *Curr. Biol.* **17**: 1055–60.

704 **Miao, J., Guo, D., Zhang, J., Huang, Q., Qin, G., Zhang, X., Wan, J., Gu, H., and Qu, L.-J.**
705 (2013). Targeted mutagenesis in rice using CRISPR-Cas system. *Cell Res.* **23**: 1233–6.

706 **Mimida, N., Kidou, S.-I., Iwanami, H., Moriya, S., Abe, K., Voogd, C., Varkonyi-Gasic, E., and**
707 **Kotoda, N.** (2011). Apple FLOWERING LOCUS T proteins interact with transcription factors
708 implicated in cell growth and organ development. *Tree Physiol.* **31**: 555–66.

709 **Muszynski, M.G., Dam, T., Li, B., Shirbroun, D.M., Hou, Z., Bruggemann, E., Archibald, R.,**
710 **Ananiev, E. V, and Danilevskaya, O.N.** (2006). delayed flowering1 Encodes a basic leucine

711 zipper protein that mediates floral inductive signals at the shoot apex in maize. *Plant Physiol.* **142**:
712 1523–1536.

713 **Navarro, C., Abelenda, J.A., Cruz-Oró, E., Cuéllar, C.A., Tamaki, S., Silva, J., Shimamoto, K.,**
714 **and Prat, S.** (2011). Control of flowering and storage organ formation in potato by FLOWERING
715 LOCUS T. *Nature* **478**: 119–122.

716 **Niwa, M., Daimon, Y., Kurotani, K., Higo, A., Pruneda-Paz, J.L., Breton, G., Mitsuda, N., Kay,**
717 **S.A., Ohme-Takagi, M., Endo, M., and Araki, T.** (2013). BRANCHED1 interacts with
718 FLOWERING LOCUS T to repress the floral transition of the axillary meristems in Arabidopsis.
719 *Plant Cell* **25**: 1228–42.

720 **Ogiso-Tanaka, E., Matsubara, K., Yamamoto, S., Nonoue, Y., Wu, J., Fujisawa, H., Ishikubo, H.,**
721 **Tanaka, T., Ando, T., Matsumoto, T., and Yano, M.** (2013). Natural Variation of the RICE
722 FLOWERING LOCUS T 1 Contributes to Flowering Time Divergence in Rice. *PLoS One* **8**:
723 e75959.

724 **Ouwerkerk, P.B., de Kam, R.J., Hoge, J.H., and Meijer, A.H.** (2001). Glucocorticoid-inducible
725 gene expression in rice. *Planta* **213**: 370–8.

726 **Park, S.J., Jiang, K., Tal, L., Yichie, Y., Gar, O., Zamir, D., Eshed, Y., and Lippman, Z.B.** (2014).
727 Optimization of crop productivity in tomato using induced mutations in the florigen pathway. *Nat.*
728 *Genet.* **46**: 1337–42.

729 **Pin, P.A., Benlloch, R., Bonnet, D., Wremerth-Weich, E., Kraft, T., Gielen, J.J.L., and Nilsson, O.**
730 (2010). An Antagonistic Pair of FT Homologs Mediates the Control of Flowering Time in Sugar
731 Beet. *Science* **330**: 1397–1400.

732 **Pnueli, L., Gutfinger, T., Hareven, D., Ben-Naim, O., Ron, N., Adir, N., and Lifschitz, E.** (2001).
733 Tomato SP-interacting proteins define a conserved signaling system that regulates shoot
734 architecture and flowering. *Plant Cell* **13**: 2687–702.

735 **Purwestri, Y.A., Ogaki, Y., Tamaki, S., Tsuji, H., and Shimamoto, K.** (2009). The 14-3-3 protein
736 GF14c acts as a negative regulator of flowering in rice by interacting with the florigen Hd3a. *Plant*
737 *Cell Physiol.* **50**: 429–438.

738 **Randoux, M., Davière, J.-M., Jeauffre, J., Thouroude, T., Pierre, S., Toualbia, Y., Perrotte, J.,**
739 **Reynoird, J.-P., Jammes, M.-J., Hibrand-Saint Oyant, L., and Foucher, F.** (2014). RoKSN, a
740 floral repressor, forms protein complexes with RoFD and RoFT to regulate vegetative and
741 reproductive development in rose. *New Phytol.* **202**: 161–173.

742 **Reinke, A.W., Baek, J., Ashenberg, O., and Keating, A.E.** (2013). Networks of bZIP protein-protein

743 interactions diversified over a billion years of evolution. *Science* **340**: 730–734.

744 **Sahoo, K.K., Tripathi, A.K., Pareek, A., Sopory, S.K., and Singla-Pareek, S.L.** (2011). An
745 improved protocol for efficient transformation and regeneration of diverse indica rice cultivars.
746 *Plant Methods* **7**: 49.

747 **Schütze, K., Harter, K., and Chaban, C.** (2008). Post-translational regulation of plant bZIP factors.
748 *Trends Plant Sci.* **13**: 247–255.

749 **Sentoku, N., Sato, Y., Kurata, N., Ito, Y., Kitano, H., and Matsuoka, M.** (1999). Regional
750 Expression of the Rice KN1-Type Homeobox Gene Family during Embryo, Shoot, and Flower
751 Development. *Plant Cell* **11**: 1651–1664.

752 **Shahmuradov, I.A. and Solovyev, V. V.** (2014). Nsite, NsiteH and NsiteM computer tools for
753 studying transcription regulatory elements. *Bioinformatics* **31**: 3544–3545.

754 **Somssich, M., Ma, Q., Weidtkamp-Peters, S., Stahl, Y., Felekyan, S., Bleckmann, A., Seidel,
755 C.A.M., and Simon, R.** (2015). Real-time dynamics of peptide ligand-dependent receptor
756 complex formation in planta. *Sci. Signal.* **8**: ra76-ra76.

757 **Soyk, S., Mueller, N.A., Park, S.J., Schmalenbach, I., Jiang, K., Hayama, R., Zhang, L., Van Eck,
758 J., Jimenez-Gomez, J.M., and Lippman, Z.B.** (2016). Variation in the flowering gene SELF
759 PRUNING 5G promotes day-neutrality and early yield in tomato. *Nat. Genet.* **49**: 162–168.

760 **Stahl, Y. et al.** (2013). Moderation of arabidopsis root stemness by CLAVATA1 and ARABIDOPSIS
761 CRINKLY4 receptor kinase complexes. *Curr. Biol.* **23**: 362–371.

762 **Sussmilch, F.C., Berbel, A., Hecht, V., Vander Schoor, J.K., Ferrándiz, C., Madueño, F., and
763 Weller, J.L.** (2015). Pea VEGETATIVE2 Is an FD Homolog That Is Essential for Flowering and
764 Compound Inflorescence Development. *Plant Cell* **27**: 1046–60.

765 **Tamaki, S., Matsuo, S., Wong, H.L., Yokoi, S., and Shimamoto, K.** (2007). Hd3a Protein Is a
766 Mobile Flowering Signal in Rice. *Science.* **316**: 1033–1036.

767 **Tamaki, S., Tsuji, H., Matsumoto, A., Fujita, A., Shimatani, Z., Terada, R., Sakamoto, T.,
768 Kurata, T., and Shimamoto, K.** (2015). FT-like proteins induce transposon silencing in the shoot
769 apex during floral induction in rice. *Proc. Natl. Acad. Sci. U. S. A.* **112**: E901-10.

770 **Tang, N. et al.** (2016). MODD mediates deactivation and degradation of OsbZIP46 to negatively
771 regulate ABA signaling and drought resistance in rice. *Plant Cell* **28**: tpc.00171.2016.

772 **Taoka, K. et al.** (2011). 14-3-3 proteins act as intracellular receptors for rice Hd3a florigen. *Nature*
773 **476**: 332–5.

774 **Teo, C.-J., Takahashi, K., Shimizu, K., Shimamoto, K., and Taoka, K.** (2017). Potato Tuber

775 Induction is Regulated by Interactions Between Components of a Tubergen Complex. *Plant Cell*
776 *Physiol.* **58**: 365–374.

777 **Teper-Bamnolker, P. and Samach, A.** (2005). The flowering integrator FT regulates SEPALLATA3
778 and FRUITFULL accumulation in Arabidopsis leaves. *Plant Cell* **17**: 2661–75.

779 **Tsuda, K., Ito, Y., Sato, Y., and Kurata, N.** (2011). Positive Autoregulation of a KNOX Gene Is
780 Essential for Shoot Apical Meristem Maintenance in Rice. *Plant Cell* **23**: 4368–4381.

781 **Tsuji, H., Nakamura, H., Taoka, K., and Shimamoto, K.** (2013). Functional diversification of FD
782 transcription factors in rice, components of florigen activation complexes. *Plant Cell Physiol.* **54**:
783 385–97.

784 **Tsuji, H., Tachibana, C., Tamaki, S., Taoka, K.-I., Kyojuka, J., and Shimamoto, K.** (2015). Hd3a
785 promotes lateral branching in rice. *Plant J.* **82**: 256–66.

786 **Tylewicz, S., Tsuji, H., Miskolczi, P., Petterle, A., Azeez, A., Jonsson, K., Shimamoto, K., and**
787 **Bhalerao, R.P.** (2015). Dual role of tree florigen activation complex component FD in
788 photoperiodic growth control and adaptive response pathways. *Proc. Natl. Acad. Sci. U. S. A.* **112**:
789 3140–5.

790 **Wickland, D. and Hanzawa, Y.** (2015). The FLOWERING LOCUS T/TERMINAL FLOWER1 Gene
791 Family: Functional Evolution and Molecular Mechanisms. *Mol. Plant* **8**: 983–997.

792 **Wigge, P.A., Kim, M.C., Jaeger, K.E., Busch, W., Schmid, M., Lohmann, J.U., and Weigel, D.**
793 (2005). Integration of spatial and temporal information during floral induction in Arabidopsis.
794 *Science* **309**: 1056–9.

795 **Wu, J., Zhu, C., Pang, J., Zhang, X., Yang, C., Xia, G., Tian, Y., and He, C.** (2014). OsLOL1, a
796 C2C2-type zinc finger protein, interacts with OsBZIP58 to promote seed germination through the
797 modulation of gibberellin biosynthesis in *Oryza sativa*. *Plant J.* **80**: 1118–1130.

798 **Zhang, C., Liu, J., Zhao, T., Gomez, A., Li, C., Yu, C., Li, H., Lin, J., Yang, Y., Liu, B., and Lin,**
799 **C.** (2016). A Drought-inducible bZIP Transcription Factor OsABF1 Delays Reproductive Timing
800 in Rice. *Plant Physiol.* **171**: 334–343.

801 **Zhao, J., Chen, H., Ren, D., Tang, H., Qiu, R., Feng, J., Long, Y., Niu, B., Chen, D., Zhong, T.,**
802 **Liu, Y.-G., and Guo, J.** (2015). Genetic interactions between diverged alleles of Early heading
803 date 1 (Ehd1) and Heading date 3a (Hd3a) / RICE FLOWERING LOCUS T1 (RFT1) control
804 differential heading and contribute to regional adaptation in rice (*Oryza sativa*). *New Phytol.*
805 **208**: 936–948.

806

807 **Figure Legends**

808 **Figure 1. Overexpression of *OsFD1* in leaves induces transcription of targets of the FAC. (A-C)**
809 Expression of *OsFD1* (A), *OsMADS14* (B) and *OsMADS15* (C) in leaves of transgenic *proACT:OsFD1*
810 plants. Plants were grown under LD (14.5 h light) for 6 weeks and then shifted to SD (10 h light). Leaves
811 were collected at ZT0 after 6 and 13 days after shift to SD (DAS, days after shift). *UBIQUITIN* (*UBQ*)
812 was used as standard for quantification of gene expression. Data are represented as mean \pm st.dev. E-n=
813 $\times 10^{-n}$. ANOVA tests for graphs in A, B and C are shown in Supplemental File 1.

814

815 **Figure 2. Expression of *OsMADS14* and *OsMADS15* in leaves is dependent upon expression of *Hd3a***
816 **and *RFT1*.** (A) Schematics of the inducible system used in this study. The GVG chimeric protein is
817 expressed under the *GOS2* promoter, to produce the inducible part of the vector. The *Hd3a* or *RFT1*
818 coding sequences are cloned under the control of the *4x UPSTREAM ACTIVATION SEQUENCE* (*UAS*),
819 to produce the effector component of the vector. T indicates the terminator. (B-E) Expression of *Hd3a*
820 (B), *RFT1* (C), *OsMADS14* (D) and *OsMADS15* (E) in leaves of DEX-inducible transgenic plants grown
821 under LD. Leaves were harvested at ZT0. *GVG:Hd3a* and *GVG:RFT1* indicate DEX-inducible *Hd3a* and
822 *RFT1* overexpressing lines, respectively. Two independent transgenic lines are shown for each construct.
823 Plants were either DEX- or mock-treated and transcripts were quantified using primers designed on the
824 coding sequences. *UBIQUITIN* (*UBQ*) was used as standard for quantification of gene expression. Data
825 are represented as mean \pm st.dev. xE-n= $\times 10^{-n}$. ANOVA tests for graphs in B, C, D and E are shown in
826 Supplemental File 1.

827

828

829 **Figure 3. A negative feedback loop independent of *OsFD1* reduces *Ehd1*, *Hd3a* and *RFT1***
830 **expression during floral induction in leaves.** (A-D) DEX-induced overexpression of *Hd3a* (A, B) or
831 *RFT1* (C, D) causes strong increase of *Hd3a* (A) or *RFT1* (C) transcript accumulation from transgenic
832 sequences, but downregulation of *Ehd1*, *Hd3a* and *RFT1* endogenous transcripts, compared to mock-
833 treated controls (B, D). (E-F) Two independent transgenic *proACT:OsFD1* lines show increased
834 expression of *OsFD1* (E) and of *Ehd1*, *Hd3a* and *RFT1* in leaves compared to the wild type (F). DEX
835 was applied at 13 DAS, and leaf samples were collected at ZT0, 16h later. *proACT:OsFD1* plants were
836 collected at ZT0 and 12 DAS. Leaves from 10 plants per treatment were sampled. *UBQ* was used as
837 standard for quantification of gene expression. Data are represented by mean \pm st.dev. Primers on *Hd3a*
838 or *RFT1* coding sequences or on the 3'UTRs were used to distinguish transgenic+endogenous (A, C)

839 from endogenous transcripts, respectively (**B**, **D**). ANOVA tests for graphs in A-F are shown in
840 Supplemental File 1.

841

842

843 **Figure 4. HBF1 and HBF2 interact with GF14c and directly with Hd3a.** (**A**) Yeast-two-hybrid assays
844 between Hd3a, RFT1 and Gf14c fused to the binding domain (BD) and HBF1 or HBF2 fused to the
845 activation domain (AD) of Gal4. Colonies were grown on selective -L-W-H medium supplemented with
846 10mM 3AT. (**B**) BiFC assays showing restored YFP fluorescence in nuclei upon co-expression of Hd3a-
847 YFP C with HBF1-YFP N, HBF2-YFP N or OsbZIP62-YFP N. Bar, 10 μ m. (**C**) FRET-FLIM
848 measurements of the Hd3a-GFP donor lifetime in the presence of the acceptors OsFD1-mCherry (no
849 FRET), HBF1-mCherry, HBF2-mCherry or OsbZIP62-mCherry. The average lifetime of 10 transformed
850 nuclei per measurement is shown \pm st. dev. An asterisk indicates significance for $p < 0.0003$ (Student's
851 t-test). (**D**) Color code indicating the lifetime of GFP at each pixel in one representative nucleus for the
852 interactions shown in (**C**). For the interaction between Hd3a and OsbZIP62 two adjacent cells are shown,
853 where only the left nucleus (arrow) co-expresses both constructs, while the right one expresses only
854 Hd3a-GFP. Accordingly, shortened lifetime is observed only in the left nucleus. (**E**) GST-pull down assay
855 showing interactions between MBP-HBF1 and MBP-HBF2 with GST-Gf14c and GST-Hd3a, but not
856 with GST alone. An immunoblot using an anti-MBP antibody is shown. Protein sizes are MBP-HBF1:
857 79.5 kDa, MBP-HBF2: 79.5 kDa. Resin loading control is shown in Supplemental Figure 3E. ANOVA
858 test for graph in C is shown in Supplemental File 1.

859

860

861 **Figure 5. HBF1 and HBF2 encode floral repressors repressing *Ehd1* expression.** (**A**, **B**)
862 Quantification of mRNA levels of *Ehd1*, *Hd3a* and *RFT1* in leaves of *proACT:HBF1* (**A**) and
863 *proACT:HBF2* (**B**) overexpression plants grown for 8 weeks under LD (16 h light) and then shifted to
864 SD (10 h light). *UBQ* was used as standard for quantification of gene expression. Data are represented
865 by mean \pm st.dev. (**C**) Days to heading of wild type, *proACT:HBF1*, *proACT:HBF2* and *proACT:OsFD1*
866 overexpressors grown for 8 weeks under LD (16 h light) and then shifted to SD (10 h light). (**D**) Heading
867 dates of wild type (Dongjin) and *hbfl-1* mutants grown under continuous LD (14.5 h light) or continuous
868 SD (10 h light). (**E-G**) Expression of *Ehd1* (**E**), *Hd3a* (**F**) and *RFT1* (**G**) in *hbfl-1* mutant plants compared
869 to the wild type. mRNA levels are shown at 10 and 17 days after shifting plants from LD to SD (**H-K**).
870 Nipponbare wild type and T2 *hbfl hbfl2* CRISPR mutants grown under continuous LD (14.5 h light) (**H**)

871 or shifted from LD (16 h light) to SD (10 h light) 8 weeks after sowing (**I**). Arrowheads indicate the
872 emerging panicles. (**J, K**) Quantification of heading dates in the same plants as in **H** and **I**, respectively
873 (n indicates the number of plants scored). Asterisks indicate $p < 0.05$ in an unpaired two tailed Student's
874 t-test. $E-n = x 10^{-n}$. The detailed genotypes of the mutants are reported in Supplemental Figure 5C.
875 ANOVA tests for graphs in A-G, J and K are shown in Supplemental File 1.

876
877

878 **Figure 6. HBF1 represses flowering at the SAM.** (**A**) Quantification of *HBF1* expression in SAMs and
879 leaves of plants misexpressing *HBF1* from the *OSHI* promoter. Two independent transgenic lines are
880 shown. (**B**) Heading dates of *proOSHI:HBF1* transgenic plants grown for 8 weeks under LD (16 h light)
881 and then shifted to SD (10 h light) (n indicates the number of plants scored). Asterisks indicate $p < 0.05$
882 in an unpaired two tailed Student's t-test. (**C**) Quantification of *OsMADS14* and *OsMADS15* expression
883 in SAMs of transgenic *proOSHI:HBF1* plants. Samples in **A** and **C** were collected from apical meristems
884 grown under LD and then exposed to 12 inductive SD. *UBQ* was used as standard for quantification of
885 gene expression. All data are represented by mean \pm st.dev. $E-n = x 10^{-n}$. (**D**) EMSA between MBP-HBF1
886 and *ABRE*-Cy5 (lanes 1-4) and HBF1 and *CArG*-box-Cy5 (lane 6). The specificity of interaction between
887 HBF1 and *ABRE*-Cy5 was tested by incubation with increasing amounts of unlabeled oligonucleotides
888 (labelled/unlabelled oligonucleotide ratios 1:2, 1:5, 1:25). HBF1 was incubated with an oligonucleotide
889 containing a *CArG*-box-Cy5 (lanes 5 and 6) as a negative control. FP, free probe. ANOVA tests for
890 graphs in A-C are shown in Supplemental File 1.

891

892 **Figure 7. Combinatorial circuitry controlling production of and response to florigenic proteins in**
893 **rice.** In leaves Hd3a and RFT1 can promote expression of *Ehd1* by forming a canonical FAC with OsFD1
894 and Gf14c, and they can repress it by interacting with HBFs. Hd3a can interact directly with HBFs,
895 whereas RFT1 might interact indirectly with HBFs through GF14c. Binding of HBF1 to the *Ehd1*
896 promoter is direct. Upon translocation to the meristem, Hd3a and RFT1 proteins can promote
897 transcription of *OsMADS* target genes by forming a canonical FAC. HBF1 at least can repress
898 transcription of the same targets by forming a repressive FAC. Gray arrows and flat-end arrows indicate
899 transcriptional activation and repression, respectively. Connectors indicate protein–protein interactions.
900 Thick, black flat-end arrows indicate direct repression by protein–DNA binding. Dashed arrows indicate
901 protein movement.

902

903 **Table 1. Targeted yeast two-hybrid analysis between Hd3a, RFT1, Gf14c and selected OsbZIPs.**
 904 Interaction strength is shown as the highest 3-amino-triazole (3AT) concentration on which diploid
 905 colonies could grow when plated on selective medium. A minus indicates no interaction. n.t., not tested.
 906 BD fusions were expressed in yeast strain Y187 (mata α) and AD fusions were expressed in yeast AH109
 907 (matA). Diploid yeast was produced by mating. Growth was observed after 6 days at 30°C.
 908
 909

	AD clones									
	Hd3a	RFT1	Gf14c	OsFD1	OsbZIP69/ OsFD4	OsbZIP24/ OsFD3	OsbZIP62	OsbZIP9/ HBF2	OsbZIP42/ HBF1	Empty AD
BD clones										
Hd3a	-	-	20	-	-	-	15	20	20	-
RFT1	-	-	20	-	-	-	-	-	-	-
Gf14c	-	-	20	20	-	15	10	20	20	-
OsFD1	-	-	10	-	-	-	-	-	n.t.	-
OsbZIP69/ OsFD4	-	-	-	-	20	20	-	-	-	-
OsbZIP24/ OsFD3	-	-	15	-	-	20	-	-	-	-
OsbZIP62	-	-	20	-	-	-	-	n.t.	-	-
OsbZIP9/ HBF2	-	-	10	-	-	-	-	n.t.	-	-
OsbZIP42/ HBF1	10	-	15	-	-	-	-	-	n.t.	-
Empty BD	-	-	-	-	-	-	-	-	-	-

910

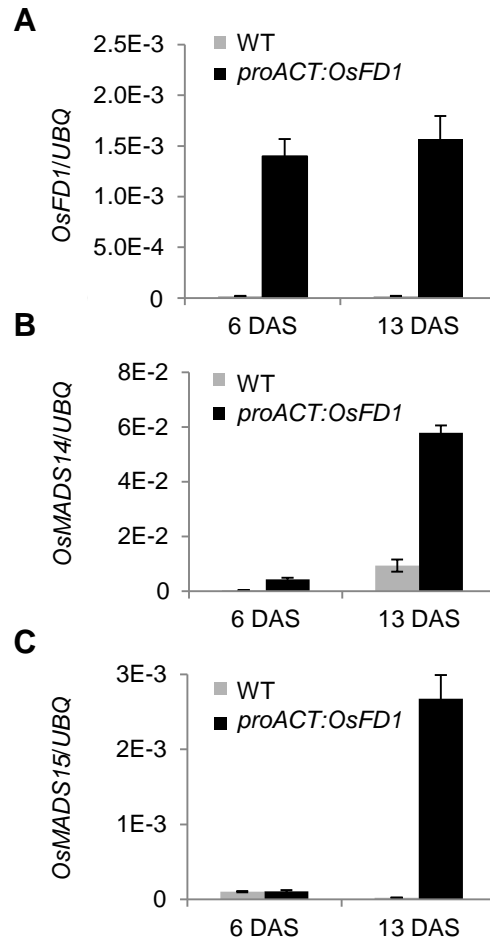


Figure 1. Overexpression of *OsFDI* in leaves induces transcription of targets of the FAC. (A-C) Expression of *OsFDI* (A), *OsMADS14* (B) and *OsMADS15* (C) in leaves of transgenic *proACT:OsFDI* plants. Plants were grown under LD (14.5 h light) for 6 weeks and then shifted to SD (10 h light). Leaves were collected at ZT0 after 6 and 13 days after shift to SD (DAS, days after shift). *UBIQUITIN (UBQ)* was used as standard for quantification of gene expression. Data are represented as mean \pm st.dev. E-n= x 10⁻ⁿ.

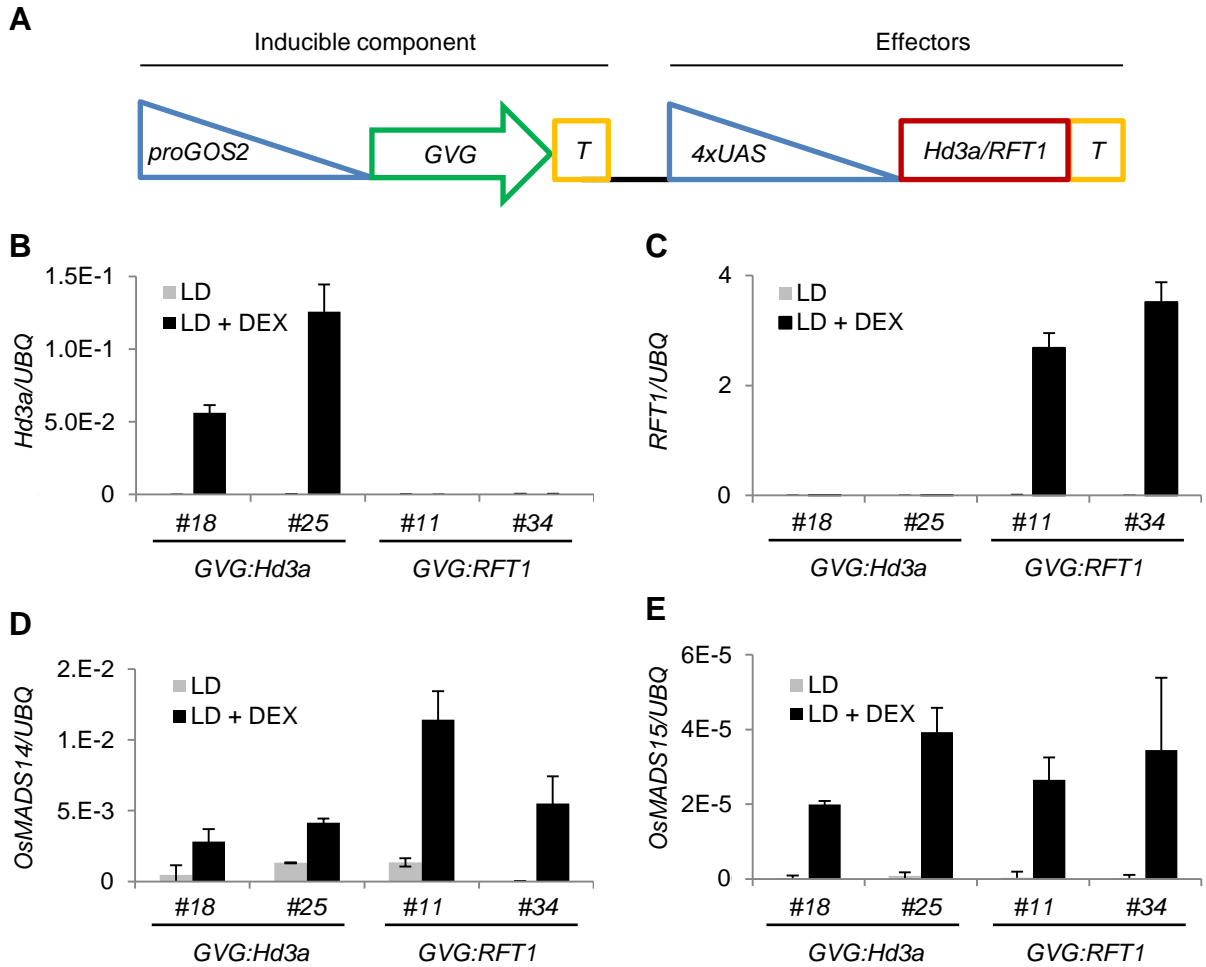


Figure 2. Expression of *OsMADS14* and *OsMADS15* in leaves is dependent upon expression of *Hd3a* and *RFT1*. (A) Schematics of the inducible system used in this study. The GVG chimeric protein is expressed under the *GOS2* promoter, to produce the inducible part of the vector. The *Hd3a* or *RFT1* coding sequences are cloned under the control of the 4x UPSTREAM ACTIVATION SEQUENCE (UAS), to produce the effector component of the vector. T indicates the terminator. (B-E) Expression of *Hd3a* (B), *RFT1* (C), *OsMADS14* (D) and *OsMADS15* (E) in leaves of DEX-inducible transgenic plants grown under LD. Leaves were harvested at ZT0. *GVG:Hd3a* and *GVG:RFT1* indicate DEX-inducible *Hd3a* and *RFT1* overexpressing lines, respectively. Two independent transgenic lines are shown for each construct. Plants were either DEX- or mock-treated and transcripts were quantified using primers designed on the coding sequences. *UBIQUITIN (UBQ)* was used as standard for quantification of gene expression. Data are represented as mean \pm st.dev. xE-n= x 10⁻ⁿ.

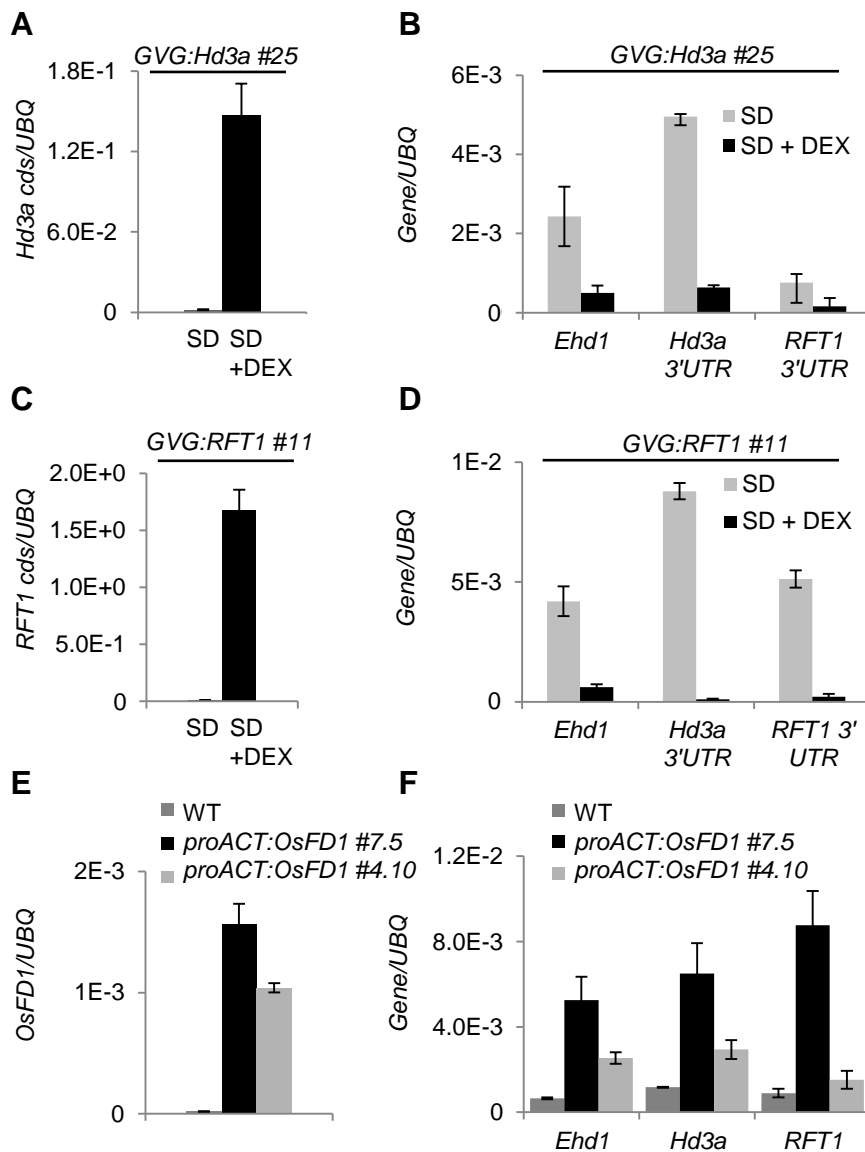


Figure 3. A negative feedback loop independent of *OsFD1* reduces *Ehd1*, *Hd3a* and *RFT1* expression during floral induction in leaves. (A-D) DEX-induced overexpression of *Hd3a* (A, B) or *RFT1* (C, D) causes strong increase of *Hd3a* (A) or *RFT1* (C) transcript accumulation from transgenic sequences, but downregulation of *Ehd1*, *Hd3a* and *RFT1* endogenous transcripts, compared to mock-treated controls (B, D). (E-F) Two independent transgenic *proACT:OsFD1* lines show increased expression of *OsFD1* (E) and of *Ehd1*, *Hd3a* and *RFT1* in leaves compared to the wild type (F). DEX was applied at 13 DAS, and leaf samples were collected at ZT0, 16h later. *proACT:OsFD1* plants were collected at ZT0 and 12 DAS. Leaves from 10 plants per treatment were sampled. *UBQ* was used as standard for quantification of gene expression. Data are represented by mean \pm st.dev. Primers on *Hd3a* or *RFT1* coding sequences or on the 3'UTRs were used to distinguish transgenic+endogenous (A, C) from endogenous transcripts, respectively (B, D).

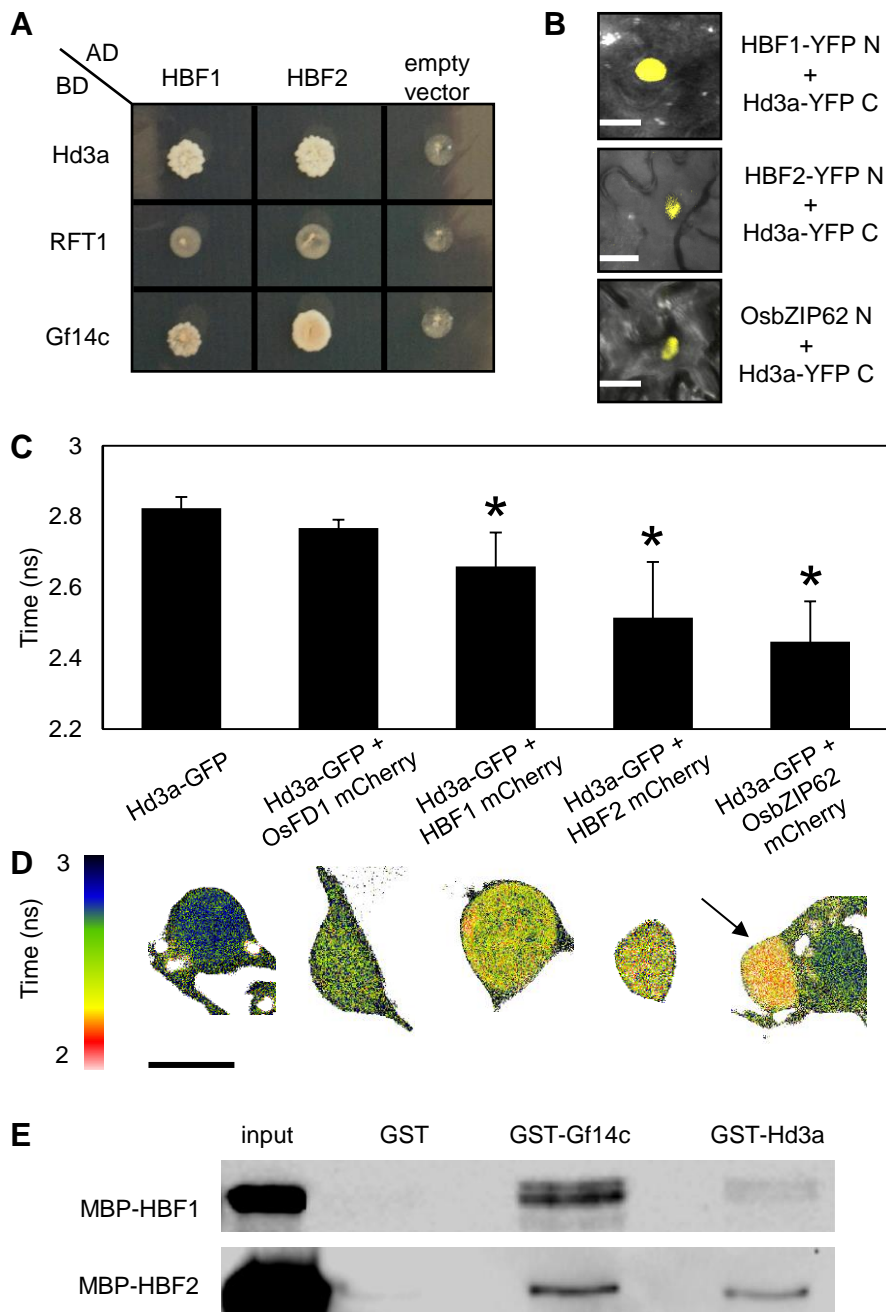


Figure 4. HBf1 and HBf2 interact with Gf14c and directly with Hd3a. (A) Yeast-two-hybrid assays between Hd3a, RFT1 and Gf14c fused to the binding domain (BD) and HBf1 or HBf2 fused to the activation domain (AD) of Gal4. Colonies were grown on selective -L-W-H medium supplemented with 10mM 3AT. (B) BiFC assays showing restored YFP fluorescence in nuclei upon co-expression of Hd3a-YFP C with HBf1-YFP N, HBf2-YFP N or OsbZIP62-YFP N. Bar, 10 μ m. (C) FRET-FLIM measurements of the Hd3a-GFP donor lifetime in the presence of the acceptors OsFD1-mCherry (no FRET), HBf1-mCherry, HBf2-mCherry or OsbZIP62-mCherry. The average lifetime of 10 transformed nuclei per measurement is shown \pm st. dev. An asterisk indicates significance for $p < 0.0003$ (Student's t-test). (D) Color code indicating the lifetime of GFP at each pixel in one representative nucleus for the interactions shown in (C). For the interaction between Hd3a and OsbZIP62 two adjacent cells are shown, where only the left nucleus (arrow) co-expresses both constructs, while the right one expresses only Hd3a-GFP. Accordingly, shortened lifetime is observed only in the left nucleus. (E) GST-pull down assay showing interactions between MBP-HBF1 and MBP-HBF2 with GST-Gf14c and GST-Hd3a, but not with GST alone. An immunoblot using an anti-MBP antibody is shown. Protein sizes are MBP-HBF1: 79.5 kDa, MBP-HBF2: 79.5 kDa. Resin loading control is shown in Supplemental Figure 3E.

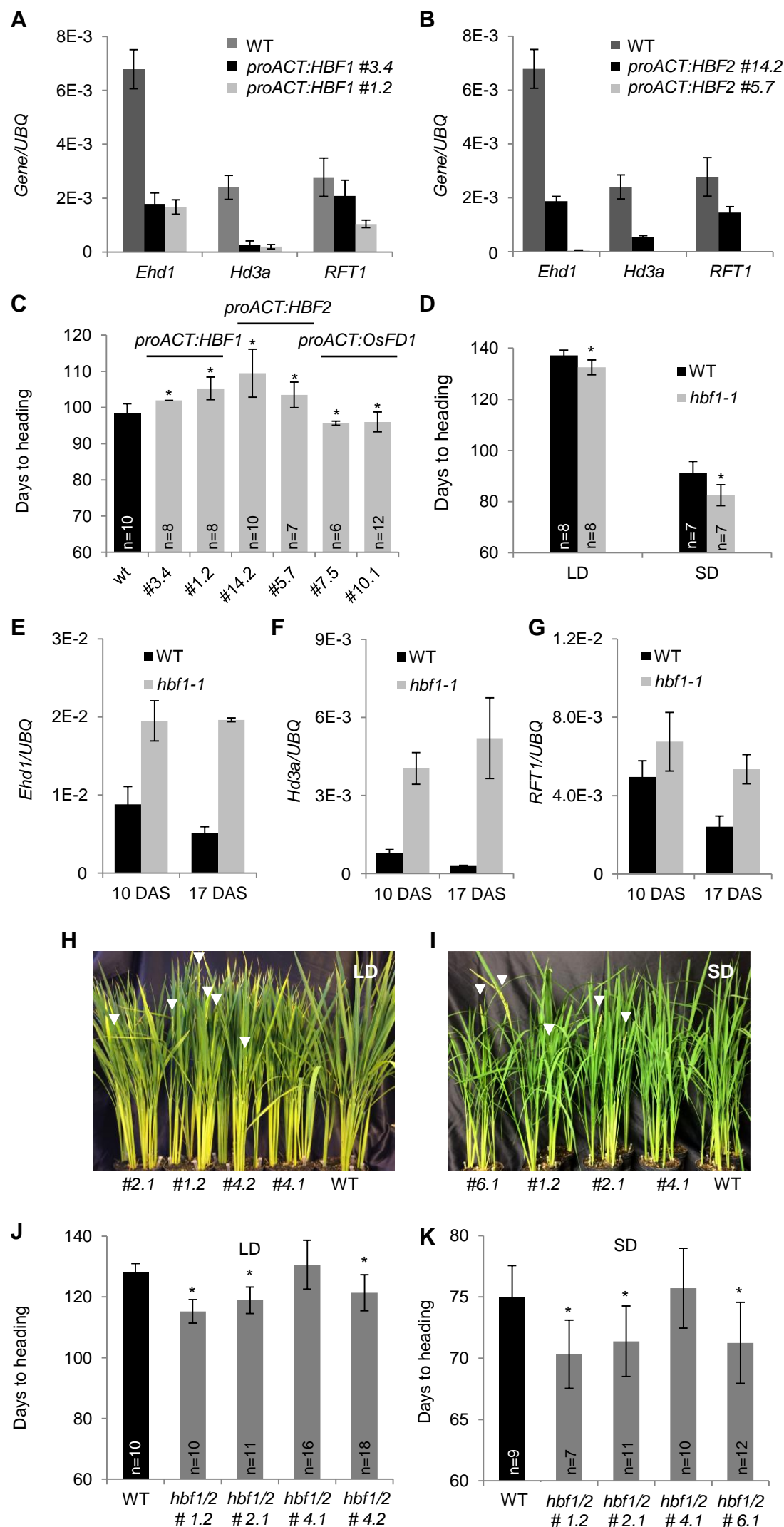


Figure 5. *HBF1* and *HBF2* encode floral repressors repressing *Ehd1* expression. (A, B) Quantification of mRNA levels of *Ehd1*, *Hd3a* and *RFT1* in leaves of *proACT:HBF1* (A) and *proACT:HBF2* (B) overexpression plants grown for 8 weeks under LD (16 h light) and then shifted to SD (10 h light). *UBQ* was used as standard for quantification of gene expression. Data are represented by mean \pm st.dev. (C) Days to heading of wild type, *proACT:HBF1*, *proACT:HBF2* and *proACT:OsFD1* overexpressors grown for 8 weeks under LD (16 h light) and then shifted to SD (10 h light). (D) Heading dates of wild type (Dongjin) and *hbf1-1* mutants grown under continuous LD (14.5 h light) or continuous SD (10 h light). (E-G) Expression of *Ehd1* (E), *Hd3a* (F) and *RFT1* (G) in *hbf1-1* mutant plants compared to the wild type. mRNA levels are shown at 10 and 17 days after shifting plants from LD to SD (H-K). Nipponbare wild type and T2 *hbf1 hbf2* CRISPR mutants grown under continuous LD (14.5 h light) (H) or shifted from LD (16 h light) to SD (10 h light) 8 weeks after sowing (I). Arrowheads indicate the emerging panicles. (J, K) Quantification of heading dates in the same plants as in H and I, respectively (n indicates the number of plants scored). Asterisks indicate $p < 0.05$ in an unpaired two tailed Student's t-test. E-n= $\times 10^{-n}$. The detailed genotypes of the mutants are reported in Supplemental Figure 5C.

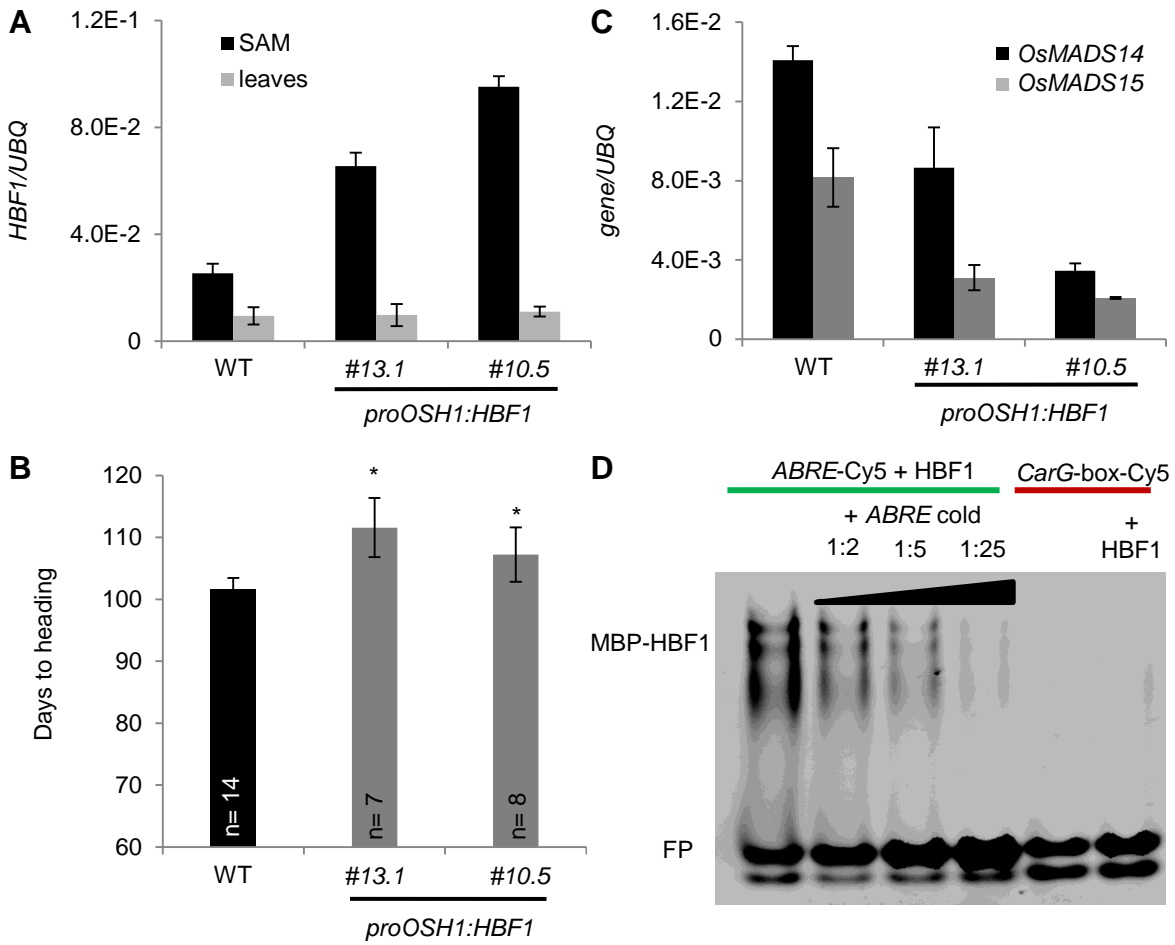


Figure 6. HBF1 represses flowering at the SAM. (A) Quantification of *HBFI* expression in SAMs and leaves of plants misexpressing *HBFI* from the *OSHI* promoter. Two independent transgenic lines are shown. (B) Heading dates of *proOSHI:HBFI* transgenic plants grown for 8 weeks under LD (16 h light) and then shifted to SD (10 h light) (n indicates the number of plants scored). Asterisks indicate $p < 0.05$ in an unpaired two tailed Student's t-test. (C) Quantification of *OsMADS14* and *OsMADS15* expression in SAMs of transgenic *proOSHI:HBFI* plants. Samples in A and C were collected from apical meristems grown under LD and then exposed to 12 inductive SD. *UBQ* was used as standard for quantification of gene expression. All data are represented by mean \pm st.dev. E-n= $x \cdot 10^{-n}$. (D) EMSA between MBP-HBF1 and ABRE-Cy5 (lanes 1-4) and HBF1 and CARG-box-Cy5 (lane 6). The specificity of interaction between HBF1 and ABRE-Cy5 was tested by incubation with increasing amounts of unlabeled oligonucleotides (labelled/unlabelled oligonucleotide ratios 1:2, 1:5, 1:25). HBF1 was incubated with an oligonucleotide containing a CARG-box-Cy5 (lanes 5 and 6) as a negative control. FP, free probe.

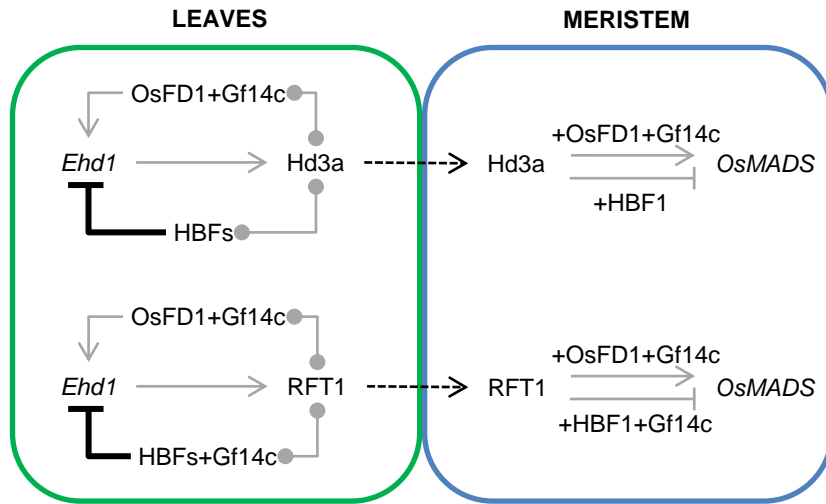


Figure 7. Combinatorial circuitry controlling production of and response to florigenic proteins in rice. In leaves Hd3a and RFT1 can promote expression of *Ehd1* by forming a canonical FAC with OsFD1 and Gf14c, and they can repress it by interacting with HBFs. Hd3a can interact directly with HBFs, whereas RFT1 might interact indirectly with HBFs through GF14c. Binding of HBF1 to the *Ehd1* promoter is direct. Upon translocation to the meristem, Hd3a and RFT1 proteins can promote transcription of *OsMADS* target genes by forming a canonical FAC. HBF1 at least can repress transcription of the same targets by forming a repressive FAC. Gray arrows and flat-end arrows indicate transcriptional activation and repression, respectively. Connectors indicate protein–protein interactions. Thick, black flat-end arrows indicate direct repression by protein–DNA binding. Dashed arrows indicate protein movement.

Parsed Citations

Abelenda, J., Cruz-Oró, E., Franco-Zorrilla, J., and Prat, S. (2016). Potato StCONSTANS-like1 Suppresses Storage Organ Formation by Directly Activating the FT-like StSP5G Repressor. *Curr. Biol.* 26: 872–881.

Pubmed: [Author and Title](#)

CrossRef: [Author and Title](#)

Google Scholar: [Author Only](#) [Title Only](#) [Author and Title](#)

Andrés, F. and Coupland, G. (2012). The genetic basis of flowering responses to seasonal cues. *Nat. Rev. Genet.* 13: 627–39.

Pubmed: [Author and Title](#)

CrossRef: [Author and Title](#)

Google Scholar: [Author Only](#) [Title Only](#) [Author and Title](#)

Berezin, M.Y. and Achilefu, S. (2010). Fluorescence Lifetime Measurements and Biological Imaging. *Chem. Rev. (Washington, DC, U. S.)* 110: 2641–2684.

Pubmed: [Author and Title](#)

CrossRef: [Author and Title](#)

Google Scholar: [Author Only](#) [Title Only](#) [Author and Title](#)

Bleckmann, A., Weidtkamp-Peters, S., Seidel, C. a M., and Simon, R. (2010). Stem cell signaling in Arabidopsis requires CRN to localize CLV2 to the plasma membrane. *Plant Physiol.* 152: 166–76.

Pubmed: [Author and Title](#)

CrossRef: [Author and Title](#)

Google Scholar: [Author Only](#) [Title Only](#) [Author and Title](#)

Brambilla, V. and Fornara, F. (2013). Molecular control of flowering in response to day length in rice. *J. Integr. Plant Biol.* 55: 410–8.

Pubmed: [Author and Title](#)

CrossRef: [Author and Title](#)

Google Scholar: [Author Only](#) [Title Only](#) [Author and Title](#)

Cho, L.-H., Yoon, J., Pasriga, R., and An, G. (2016). Homodimerization of Ehd1 is required to induce flowering in rice. *Plant Physiol.* 170: pp.01723.2015.

Pubmed: [Author and Title](#)

CrossRef: [Author and Title](#)

Google Scholar: [Author Only](#) [Title Only](#) [Author and Title](#)

Choi, H., Park, H.-J., Park, J.H., Kim, S., Im, M.-Y., Seo, H.-H., Kim, Y.-W., Hwang, I., and Kim, S.Y. (2005). Arabidopsis calcium-dependent protein kinase AtCPK32 interacts with ABF4, a transcriptional regulator of abscisic acid-responsive gene expression, and modulates its activity. *Plant Physiol.* 139: 1750–1761.

Pubmed: [Author and Title](#)

CrossRef: [Author and Title](#)

Google Scholar: [Author Only](#) [Title Only](#) [Author and Title](#)

Corbesier, L., Vincent, C., Jang, S., Fornara, F., Fan, Q., Searle, I., Giakountis, A., Farrona, S., Gissot, L., Turnbull, C., and Coupland, G. (2007). FT Protein Movement Contributes to Long-Distance Signaling in Floral Induction of Arabidopsis. *Science* 316: 1030–1033.

Pubmed: [Author and Title](#)

CrossRef: [Author and Title](#)

Google Scholar: [Author Only](#) [Title Only](#) [Author and Title](#)

Danilevskaya, O.N., Meng, X., Hou, Z., Ananiev, E. V., and Simmons, C.R. (2008). A Genomic and Expression Compendium of the Expanded PEBP Gene Family from Maize. *Plant Physiol.* 146: 250–264.

Pubmed: [Author and Title](#)

CrossRef: [Author and Title](#)

Google Scholar: [Author Only](#) [Title Only](#) [Author and Title](#)

Doi, K., Izawa, T., Fuse, T., Yamanouchi, U., Kubo, T., Shimatani, Z., Yano, M., and Yoshimura, A. (2004). Ehd1, a B-type response regulator in rice, confers short-day promotion of flowering and controls FT-like gene expression independently of Hd1. *Genes Dev.* 18: 926–36.

Pubmed: [Author and Title](#)

CrossRef: [Author and Title](#)

Google Scholar: [Author Only](#) [Title Only](#) [Author and Title](#)

Furihata, T., Maruyama, K., Fujita, Y., Umezawa, T., Yoshida, R., Shinozaki, K., and Yamaguchi-Shinozaki, K. (2006). Abscisic acid-dependent multisite phosphorylation regulates the activity of a transcription activator AREB1. *Proc Natl Acad Sci U S A* 103: 1988–1993.

Pubmed: [Author and Title](#)

CrossRef: [Author and Title](#)

Google Scholar: [Author Only](#) [Title Only](#) [Author and Title](#)

Galbiati, F., Chiozzotto, R., Locatelli, F., Spada, A., Genga, A., and Fornara, F. (2016). Hd3a , RFT1 and Ehd1 integrate photoperiodic and drought stress signals to delay the floral transition in rice. *Plant. Cell Environ.* 39: 1982–1993.

Pubmed: [Author and Title](#)

CrossRef: [Author and Title](#)

Google Scholar: [Author Only](#) [Title Only](#) [Author and Title](#)

Gómez-Ariza, J., Galbiati, F., Goretta, D., Brambilla, V., Shrestha, R., Pappolla, A., Courtois, B., and Fornara, F. (2015). Loss of floral repressor function adapts rice to higher latitudes in Europe. *J. Exp. Bot.* 66: 2027–39.

Pubmed: [Author and Title](#)

CrossRef: [Author and Title](#)

Google Scholar: [Author Only](#) [Title Only](#) [Author and Title](#)

Goretta, D., Martignago, D., Landini, M., Brambilla, V., Gomez-Ariza, J., Gnesutta, N., Galbiati, F., Collani, S., Takagi, H., Terauchi, R., Mantovani, R., and Fornara, F. (2017). Transcriptional and post-transcriptional mechanisms limit Heading Date 1 (Hd1) function to adapt rice to high latitudes. *PLoS Genet.* 13: e1006530.

Pubmed: [Author and Title](#)

CrossRef: [Author and Title](#)

Google Scholar: [Author Only](#) [Title Only](#) [Author and Title](#)

Hanano, S. and Goto, K. (2011). Arabidopsis TERMINAL FLOWER1 is involved in the regulation of flowering time and inflorescence development through transcriptional repression. *Plant Cell* 23: 3172–84.

Pubmed: [Author and Title](#)

CrossRef: [Author and Title](#)

Google Scholar: [Author Only](#) [Title Only](#) [Author and Title](#)

Higuchi, Y., Narumi, T., Oda, A., Nakano, Y., Sumitomo, K., Fukai, S., and Hisamatsu, T. (2013). The gated induction system of a systemic floral inhibitor, antiflorigen, determines obligate short-day flowering in chrysanthemums. *Proc. Natl. Acad. Sci.* 110: 17137–17142.

Pubmed: [Author and Title](#)

CrossRef: [Author and Title](#)

Google Scholar: [Author Only](#) [Title Only](#) [Author and Title](#)

Ho, W.W.H. and Weigel, D. (2014). Structural features determining flower-promoting activity of Arabidopsis FLOWERING LOCUS T. *Plant Cell* 26: 552–64.

Pubmed: [Author and Title](#)

CrossRef: [Author and Title](#)

Google Scholar: [Author Only](#) [Title Only](#) [Author and Title](#)

Hsu, C.-Y. et al. (2011). FLOWERING LOCUS T duplication coordinates reproductive and vegetative growth in perennial poplar. *Proc. Natl. Acad. Sci. U. S. A.* 108: 10756–61.

Pubmed: [Author and Title](#)

CrossRef: [Author and Title](#)

Google Scholar: [Author Only](#) [Title Only](#) [Author and Title](#)

Itoh, J.I., Kitano, H., Matsuoka, M., and Nagato, Y. (2000). Shoot organization genes regulate shoot apical meristem organization and the pattern of leaf primordium initiation in rice. *Plant Cell* 12: 2161–74.

Pubmed: [Author and Title](#)

CrossRef: [Author and Title](#)

Google Scholar: [Author Only](#) [Title Only](#) [Author and Title](#)

Izawa, T., Foster, R., and Chua, N.H. (1993). Plant bZIP protein DNA binding specificity. *J. Mol. Biol.* 230: 1131–1144.

Pubmed: [Author and Title](#)

CrossRef: [Author and Title](#)

Google Scholar: [Author Only](#) [Title Only](#) [Author and Title](#)

Jang, S., Choi, S.C., Li, H.Y., An, G., and Schmelzer, E. (2015). Functional characterization of phalaenopsis aphrodite flowering genes PaFT1 and PaFD. *PLoS One* 10.

Pubmed: [Author and Title](#)

CrossRef: [Author and Title](#)

Google Scholar: [Author Only](#) [Title Only](#) [Author and Title](#)

Jang, S., Li, H.-Y., and Kuo, M.-L. (2017). Ectopic expression of Arabidopsis FD and FD PARALOGUE in rice results in dwarfism with size reduction of spikelets. *Sci. Rep.* 7: 44477.

Pubmed: [Author and Title](#)

CrossRef: [Author and Title](#)

Google Scholar: [Author Only](#) [Title Only](#) [Author and Title](#)

Jaudal, M., Zhang, L., Che, C., and Putterill, J. (2015). Three Medicago MtFUL genes have distinct and overlapping expression patterns during vegetative and reproductive development and 35S:MtFULb accelerates flowering and causes a terminal flower phenotype in Arabidopsis. *Front. Genet.* 6: 50.

Pubmed: [Author and Title](#)

CrossRef: [Author and Title](#)

Google Scholar: [Author Only](#) [Title Only](#) [Author and Title](#)

Jeon, J.S. et al. (2000). T-DNA insertional mutagenesis for functional genomics in rice. *Plant J.* 22: 561–570.

Pubmed: [Author and Title](#)

CrossRef: [Author and Title](#)

Google Scholar: [Author Only](#) [Title Only](#) [Author and Title](#)

Kagaya, Y., Hobo, T., Murata, M., Ban, A., and Hattori, T. (2002). Abscisic acid-induced transcription is mediated by phosphorylation of an abscisic acid response element binding factor, TRAB1. *Plant Cell* 14: 3177–89.

Pubmed: [Author and Title](#)

CrossRef: [Author and Title](#)
Google Scholar: [Author Only Title Only Author and Title](#)

Kinoshita, T., Ono, N., Hayashi, Y., Morimoto, S., Nakamura, S., Soda, M., Kato, Y., Ohnishi, M., Nakano, T., Inoue, S.I., and Shimazaki, K.I. (2011). FLOWERING LOCUS T regulates stomatal opening. *Curr. Biol.* 21: 1232–1238.

Pubmed: [Author and Title](#)
CrossRef: [Author and Title](#)
Google Scholar: [Author Only Title Only Author and Title](#)

Kobayashi, K., Yasuno, N., Sato, Y., Yoda, M., Yamazaki, R., Kimizu, M., Yoshida, H., Nagamura, Y., and Kyojuka, J. (2012). Inflorescence Meristem Identity in Rice Is Specified by Overlapping Functions of Three AP1/FUL-Like MADS Box Genes and PAP2, a SEPALLATA MADS Box Gene. *Plant Cell* 24: 1848–1859.

Pubmed: [Author and Title](#)
CrossRef: [Author and Title](#)
Google Scholar: [Author Only Title Only Author and Title](#)

Kojima, S., Takahashi, Y., Kobayashi, Y., Monna, L., Sasaki, T., Araki, T., and Yanos, M. (2002). Hd3a, a rice ortholog of the Arabidopsis FT gene, promotes transition to flowering downstream of Hd1 under short-day conditions. *Plant Cell Physiol.* 43: 1096–105.

Pubmed: [Author and Title](#)
CrossRef: [Author and Title](#)
Google Scholar: [Author Only Title Only Author and Title](#)

Koniya, R., Ikegami, A., Tamaki, S., Yokoi, S., and Shimamoto, K. (2008). Hd3a and RFT1 are essential for flowering in rice. *Development* 135: 767–774.

Pubmed: [Author and Title](#)
CrossRef: [Author and Title](#)
Google Scholar: [Author Only Title Only Author and Title](#)

Koniya, R., Yokoi, S., and Shimamoto, K. (2009). A gene network for long-day flowering activates RFT1 encoding a mobile flowering signal in rice. *Development* 136: 3443–3450.

Pubmed: [Author and Title](#)
CrossRef: [Author and Title](#)
Google Scholar: [Author Only Title Only Author and Title](#)

Lee, R., Baldwin, S., Kenel, F., McCallum, J., and Macknight, R. (2013). FLOWERING LOCUS T genes control onion bulb formation and flowering. *Nat. Commun.* 4: 2884.

Pubmed: [Author and Title](#)
CrossRef: [Author and Title](#)
Google Scholar: [Author Only Title Only Author and Title](#)

Li, C. and Dubcovsky, J. (2008). Wheat FT protein regulates VRN1 transcription through interactions with FDL2. *Plant J.* 55: 543–554.

Pubmed: [Author and Title](#)
CrossRef: [Author and Title](#)
Google Scholar: [Author Only Title Only Author and Title](#)

Li, C., Lin, H., and Dubcovsky, J. (2015). Factorial combinations of protein interactions generate a multiplicity of florigen activation complexes in wheat and barley. *Plant J.* 84: 70–82.

Pubmed: [Author and Title](#)
CrossRef: [Author and Title](#)
Google Scholar: [Author Only Title Only Author and Title](#)

Lifschitz, E., Eviatar, T., Rozman, A., Shalit, A., Goldshmidt, A., Amsellem, Z., Alvarez, J.P., and Eshed, Y. (2006). The tomato FT ortholog triggers systemic signals that regulate growth and flowering and substitute for diverse environmental stimuli. *Proc Natl Acad Sci U S A* 103: 6398–6403.

Pubmed: [Author and Title](#)
CrossRef: [Author and Title](#)
Google Scholar: [Author Only Title Only Author and Title](#)

Litt, A and Irish, V.F. (2003). Duplication and Diversification in the APETALA1/FRUITFULL Floral Homeotic Gene Lineage: Implications for the Evolution of Floral Development. *Genetics* 165: 821–833.

Pubmed: [Author and Title](#)
CrossRef: [Author and Title](#)
Google Scholar: [Author Only Title Only Author and Title](#)

Mathieu, J., Warthmann, N., Küttner, F., and Schmid, M. (2007). Export of FT protein from phloem companion cells is sufficient for floral induction in Arabidopsis. *Curr. Biol.* 17: 1055–60.

Pubmed: [Author and Title](#)
CrossRef: [Author and Title](#)
Google Scholar: [Author Only Title Only Author and Title](#)

Miao, J., Guo, D., Zhang, J., Huang, Q., Qin, G., Zhang, X., Wan, J., Gu, H., and Qu, L.-J. (2013). Targeted mutagenesis in rice using CRISPR-Cas system. *Cell Res.* 23: 1233–6.

Pubmed: [Author and Title](#)
CrossRef: [Author and Title](#)
Google Scholar: [Author Only Title Only Author and Title](#)

Mimida, N., Kidou, S.-I., Iwanami, H., Moriya, S., Abe, K., Voogd, C., Varkonyi-Gasic, E., and Kotoda, N. (2011). Apple FLOWERING LOCUS T proteins interact with transcription factors implicated in cell growth and organ development. *Tree Physiol.* 31: 555–66.

Pubmed: [Author and Title](#)

CrossRef: [Author and Title](#)

Google Scholar: [Author Only Title Only Author and Title](#)

Muszynski, M.G., Dam, T., Li, B., Shirbroun, D.M., Hou, Z., Bruggemann, E., Archibald, R., Ananiev, E. V, and Danilevskaya, O.N. (2006). *delayed flowering1* Encodes a basic leucine zipper protein that mediates floral inductive signals at the shoot apex in maize. *Plant Physiol.* 142: 1523–1536.

Pubmed: [Author and Title](#)

CrossRef: [Author and Title](#)

Google Scholar: [Author Only Title Only Author and Title](#)

Navarro, C., Abelenda, J.A., Cruz-Oró, E., Cuéllar, C.A., Tamaki, S., Silva, J., Shimamoto, K., and Prat, S. (2011). Control of flowering and storage organ formation in potato by FLOWERING LOCUS T. *Nature* 478: 119–122.

Pubmed: [Author and Title](#)

CrossRef: [Author and Title](#)

Google Scholar: [Author Only Title Only Author and Title](#)

Niwa, M., Daimon, Y., Kurotani, K., Higo, A., Pruneda-Paz, J.L., Breton, G., Mitsuda, N., Kay, S.A., Ohme-Takagi, M., Endo, M., and Araki, T. (2013). BRANCHED1 interacts with FLOWERING LOCUS T to repress the floral transition of the axillary meristems in Arabidopsis. *Plant Cell* 25: 1228–42.

Pubmed: [Author and Title](#)

CrossRef: [Author and Title](#)

Google Scholar: [Author Only Title Only Author and Title](#)

Ogiso-Tanaka, E., Matsubara, K., Yamamoto, S., Nonoue, Y., Wu, J., Fujisawa, H., Ishikubo, H., Tanaka, T., Ando, T., Matsumoto, T., and Yano, M. (2013). Natural Variation of the RICE FLOWERING LOCUS T 1 Contributes to Flowering Time Divergence in Rice. *PLoS One* 8: e75959.

Pubmed: [Author and Title](#)

CrossRef: [Author and Title](#)

Google Scholar: [Author Only Title Only Author and Title](#)

Ouwerkerk, P.B., de Kam, R.J., Hoge, J.H., and Meijer, A.H. (2001). Glucocorticoid-inducible gene expression in rice. *Planta* 213: 370–8.

Pubmed: [Author and Title](#)

CrossRef: [Author and Title](#)

Google Scholar: [Author Only Title Only Author and Title](#)

Park, S.J., Jiang, K., Tal, L., Yichie, Y., Gar, O., Zamir, D., Eshed, Y., and Lippman, Z.B. (2014). Optimization of crop productivity in tomato using induced mutations in the florigen pathway. *Nat. Genet.* 46: 1337–42.

Pubmed: [Author and Title](#)

CrossRef: [Author and Title](#)

Google Scholar: [Author Only Title Only Author and Title](#)

Pin, P.A., Benlloch, R., Bonnet, D., Wremmerth-Weich, E., Kraft, T., Gielen, J.J.L., and Nilsson, O. (2010). An Antagonistic Pair of FT Homologs Mediates the Control of Flowering Time in Sugar Beet. *Science* 330: 1397–1400.

Pubmed: [Author and Title](#)

CrossRef: [Author and Title](#)

Google Scholar: [Author Only Title Only Author and Title](#)

Pnueli, L., Gutfinger, T., Hareven, D., Ben-Naim, O., Ron, N., Adir, N., and Lifschitz, E. (2001). Tomato SP-interacting proteins define a conserved signaling system that regulates shoot architecture and flowering. *Plant Cell* 13: 2687–702.

Pubmed: [Author and Title](#)

CrossRef: [Author and Title](#)

Google Scholar: [Author Only Title Only Author and Title](#)

Purwestri, Y.A., Ogaki, Y., Tamaki, S., Tsuji, H., and Shimamoto, K. (2009). The 14-3-3 protein GF14c acts as a negative regulator of flowering in rice by interacting with the florigen Hd3a. *Plant Cell Physiol.* 50: 429–438.

Pubmed: [Author and Title](#)

CrossRef: [Author and Title](#)

Google Scholar: [Author Only Title Only Author and Title](#)

Randoux, M., Davière, J.-M., Jeaufré, J., Thouroude, T., Pierre, S., Toulbia, Y., Perrotte, J., Reynoird, J.-P., Jammès, M.-J., Hibrand-Saint Oyant, L., and Foucher, F. (2014). RoKSN, a floral repressor, forms protein complexes with RoFD and RoFT to regulate vegetative and reproductive development in rose. *New Phytol.* 202: 161–173.

Pubmed: [Author and Title](#)

CrossRef: [Author and Title](#)

Google Scholar: [Author Only Title Only Author and Title](#)

Reinke, A.W., Baek, J., Ashenberg, O., and Keating, A.E. (2013). Networks of bZIP protein-protein interactions diversified over a billion years of evolution. *Science* 340: 730–734.

Pubmed: [Author and Title](#)

CrossRef: [Author and Title](#)

Google Scholar: [Author Only Title Only Author and Title](#)

Sahoo, K.K., Tripathi, A.K., Pareek, A., Sopory, S.K., and Singla-Pareek, S.L. (2011). An improved protocol for efficient transformation and regeneration of diverse indica rice cultivars. *Plant Methods* 7: 49.

Pubmed: [Author and Title](#)

CrossRef: [Author and Title](#)

Google Scholar: [Author Only Title Only Author and Title](#)

Schütze, K., Harter, K., and Chaban, C. (2008). Post-translational regulation of plant bZIP factors. *Trends Plant Sci.* 13: 247–255.

Pubmed: [Author and Title](#)

CrossRef: [Author and Title](#)

Google Scholar: [Author Only Title Only Author and Title](#)

Sentoku, N., Sato, Y., Kurata, N., Ito, Y., Kitano, H., and Matsuoka, M. (1999). Regional Expression of the Rice KN1-Type Homeobox Gene Family during Embryo, Shoot, and Flower Development. *Plant Cell* 11: 1651–1664.

Pubmed: [Author and Title](#)

CrossRef: [Author and Title](#)

Google Scholar: [Author Only Title Only Author and Title](#)

Shahmuradov, I.A and Solovyev, V. V. (2014). Nsite, NsiteH and NsiteM computer tools for studying transcription regulatory elements. *Bioinformatics* 31: 3544–3545.

Pubmed: [Author and Title](#)

CrossRef: [Author and Title](#)

Google Scholar: [Author Only Title Only Author and Title](#)

Somssich, M., Ma, Q., Weidtkamp-Peters, S., Stahl, Y., Felekyan, S., Bleckmann, A., Seidel, C.A.M., and Simon, R. (2015). Real-time dynamics of peptide ligand-dependent receptor complex formation in planta. *Sci. Signal.* 8: ra76-ra76.

Pubmed: [Author and Title](#)

CrossRef: [Author and Title](#)

Google Scholar: [Author Only Title Only Author and Title](#)

Soyk, S., Mueller, N.A, Park, S.J., Schmalenbach, I., Jiang, K., Hayama, R., Zhang, L., Van Eck, J., Jimenez-Gomez, J.M., and Lippman, Z.B. (2016). Variation in the flowering gene SELF PRUNING 5G promotes day-neutrality and early yield in tomato. *Nat. Genet.* 49: 162–168.

Pubmed: [Author and Title](#)

CrossRef: [Author and Title](#)

Google Scholar: [Author Only Title Only Author and Title](#)

Stahl, Y. et al. (2013). Moderation of arabidopsis root stemness by CLAVATA1 and ARABIDOPSIS CRINKLY4 receptor kinase complexes. *Curr. Biol.* 23: 362–371.

Pubmed: [Author and Title](#)

CrossRef: [Author and Title](#)

Google Scholar: [Author Only Title Only Author and Title](#)

Sussmilch, F.C., Berbel, A., Hecht, V., Vander Schoor, J.K., Ferrándiz, C., Madueño, F., and Weller, J.L. (2015). Pea VEGETATIVE2 Is an FD Homolog That Is Essential for Flowering and Compound Inflorescence Development. *Plant Cell* 27: 1046–60.

Pubmed: [Author and Title](#)

CrossRef: [Author and Title](#)

Google Scholar: [Author Only Title Only Author and Title](#)

Tamaki, S., Matsuo, S., Wong, H.L., Yokoi, S., and Shimamoto, K. (2007). Hd3a Protein Is a Mobile Flowering Signal in Rice. *Science*. 316: 1033–1036.

Pubmed: [Author and Title](#)

CrossRef: [Author and Title](#)

Google Scholar: [Author Only Title Only Author and Title](#)

Tamaki, S., Tsuji, H., Matsumoto, A., Fujita, A., Shimatani, Z., Terada, R., Sakamoto, T., Kurata, T., and Shimamoto, K. (2015). FT-like proteins induce transposon silencing in the shoot apex during floral induction in rice. *Proc. Natl. Acad. Sci. U. S. A.* 112: E901-10.

Pubmed: [Author and Title](#)

CrossRef: [Author and Title](#)

Google Scholar: [Author Only Title Only Author and Title](#)

Tang, N. et al. (2016). MODD mediates deactivation and degradation of OsbZIP46 to negatively regulate ABA signaling and drought resistance in rice. *Plant Cell* 28: tpc.00171.2016.

Pubmed: [Author and Title](#)

CrossRef: [Author and Title](#)

Google Scholar: [Author Only Title Only Author and Title](#)

Taoka, K. et al. (2011). 14-3-3 proteins act as intracellular receptors for rice Hd3a florigen. *Nature* 476: 332–5.

Pubmed: [Author and Title](#)

CrossRef: [Author and Title](#)

Google Scholar: [Author Only Title Only Author and Title](#)

Teo, C.-J., Takahashi, K., Shimizu, K., Shimamoto, K., and Taoka, K. (2017). Potato Tuber Induction is Regulated by Interactions Between Components of a Tuberigen Complex. *Plant Cell Physiol.* 58: 365–374.

Pubmed: [Author and Title](#)

CrossRef: [Author and Title](#)

Google Scholar: [Author Only Title Only Author and Title](#)

Teper-Bamnlker, P. and Samach, A. (2005). The flowering integrator FT regulates SEPALLATA3 and FRUITFULL accumulation in Arabidopsis leaves. *Plant Cell* 17: 2661–75.

Pubmed: [Author and Title](#)

CrossRef: [Author and Title](#)

Google Scholar: [Author Only Title Only Author and Title](#)

Tsuda, K., Ito, Y., Sato, Y., and Kurata, N. (2011). Positive Autoregulation of a KNOX Gene Is Essential for Shoot Apical Meristem Maintenance in Rice. *Plant Cell* 23: 4368–4381.

Pubmed: [Author and Title](#)

CrossRef: [Author and Title](#)

Google Scholar: [Author Only Title Only Author and Title](#)

Tsuji, H., Nakamura, H., Taoka, K., and Shimamoto, K. (2013). Functional diversification of FD transcription factors in rice, components of florigen activation complexes. *Plant Cell Physiol.* 54: 385–97.

Pubmed: [Author and Title](#)

CrossRef: [Author and Title](#)

Google Scholar: [Author Only Title Only Author and Title](#)

Tsuji, H., Tachibana, C., Tamaki, S., Taoka, K.-I., Kyojuka, J., and Shimamoto, K. (2015). Hd3a promotes lateral branching in rice. *Plant J.* 82: 256–66.

Pubmed: [Author and Title](#)

CrossRef: [Author and Title](#)

Google Scholar: [Author Only Title Only Author and Title](#)

Tylewicz, S., Tsuji, H., Miskolczi, P., Petterle, A., Azeez, A., Jonsson, K., Shimamoto, K., and Bhalerao, R.P. (2015). Dual role of tree florigen activation complex component FD in photoperiodic growth control and adaptive response pathways. *Proc. Natl. Acad. Sci. U. S. A.* 112: 3140–5.

Pubmed: [Author and Title](#)

CrossRef: [Author and Title](#)

Google Scholar: [Author Only Title Only Author and Title](#)

Wickland, D. and Hanzawa, Y. (2015). The FLOWERING LOCUS T/TERMINAL FLOWER1 Gene Family: Functional Evolution and Molecular Mechanisms. *Mol. Plant* 8: 983–997.

Pubmed: [Author and Title](#)

CrossRef: [Author and Title](#)

Google Scholar: [Author Only Title Only Author and Title](#)

Wigge, P.A., Kim, M.C., Jaeger, K.E., Busch, W., Schmid, M., Lohmann, J.U., and Weigel, D. (2005). Integration of spatial and temporal information during floral induction in Arabidopsis. *Science* 309: 1056–9.

Pubmed: [Author and Title](#)

CrossRef: [Author and Title](#)

Google Scholar: [Author Only Title Only Author and Title](#)

Wu, J., Zhu, C., Pang, J., Zhang, X., Yang, C., Xia, G., Tian, Y., and He, C. (2014). OsLOL1, a C2C2-type zinc finger protein, interacts with OsbZIP58 to promote seed germination through the modulation of gibberellin biosynthesis in *Oryza sativa*. *Plant J.* 80: 1118–1130.

Pubmed: [Author and Title](#)

CrossRef: [Author and Title](#)

Google Scholar: [Author Only Title Only Author and Title](#)

Zhang, C., Liu, J., Zhao, T., Gomez, A., Li, C., Yu, C., Li, H., Lin, J., Yang, Y., Liu, B., and Lin, C. (2016). A Drought-inducible bZIP Transcription Factor OsABF1 Delays Reproductive Timing in Rice. *Plant Physiol.* 171: 334–343.

Pubmed: [Author and Title](#)

CrossRef: [Author and Title](#)

Google Scholar: [Author Only Title Only Author and Title](#)

Zhao, J., Chen, H., Ren, D., Tang, H., Qiu, R., Feng, J., Long, Y., Niu, B., Chen, D., Zhong, T., Liu, Y.-G., and Guo, J. (2015). Genetic interactions between diverged alleles of Early heading date 1 (Ehd1) and Heading date 3a (Hd3a) / RICE FLOWERING LOCUS T1 (RFT1) control differential heading and contribute to regional adaptation in rice (*Oryza sativa*). *New Phytol.* 208: 936–948.

Pubmed: [Author and Title](#)

CrossRef: [Author and Title](#)

Google Scholar: [Author Only Title Only Author and Title](#)

Antagonistic Transcription Factor Complexes Modulate the Floral Transition in Rice
Vittoria Brambilla, Damiano Martignago, Daniela Goretti, Martina Cerise, Marc Somssich, Matteo de Rosa, Francesca Galbiati, Roshi Shrestha, Federico Lazzaro, Rüdiger Simon and Fabio Fornara
Plant Cell; originally published online October 17, 2017;
DOI 10.1105/tpc.17.00645

This information is current as of November 6, 2017

Supplemental Data	/content/suppl/2017/10/17/tpc.17.00645.DC1.html
Permissions	https://www.copyright.com/ccc/openurl.do?sid=pd_hw1532298X&issn=1532298X&WT.mc_id=pd_hw1532298X
eTOCs	Sign up for eTOCs at: http://www.plantcell.org/cgi/alerts/ctmain
CiteTrack Alerts	Sign up for CiteTrack Alerts at: http://www.plantcell.org/cgi/alerts/ctmain
Subscription Information	Subscription Information for <i>The Plant Cell</i> and <i>Plant Physiology</i> is available at: http://www.aspb.org/publications/subscriptions.cfm